

Green Chemistry

Accepted Manuscript



This is an *Accepted Manuscript*, which has been through the Royal Society of Chemistry peer review process and has been accepted for publication.

Accepted Manuscripts are published online shortly after acceptance, before technical editing, formatting and proof reading. Using this free service, authors can make their results available to the community, in citable form, before we publish the edited article. We will replace this *Accepted Manuscript* with the edited and formatted *Advance Article* as soon as it is available.

You can find more information about *Accepted Manuscripts* in the [Information for Authors](#).

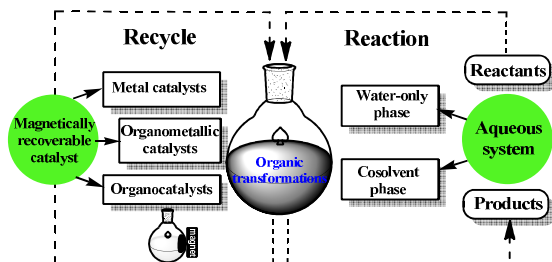
Please note that technical editing may introduce minor changes to the text and/or graphics, which may alter content. The journal's standard [Terms & Conditions](#) and the [Ethical guidelines](#) still apply. In no event shall the Royal Society of Chemistry be held responsible for any errors or omissions in this *Accepted Manuscript* or any consequences arising from the use of any information it contains.



www.rsc.org/greenchem

Magnetically recoverable nanoparticles as efficient catalysts for organic transformations in aqueous medium

Tanyu Cheng, Dacheng Zhang, Hexing Li and Guohua Liu*



This review focuses on the development of magnetically recoverable nanoparticles as efficient catalysts for organic transformations in aqueous medium.

Magnetically recoverable nanoparticles as efficient catalysts for organic transformations in aqueous medium

Cite this: DOI: 10.1039/x0xx00000x

Received 00th January 2012,
Accepted 00th January 2012

DOI: 10.1039/x0xx00000x

www.rsc.org/

Tanyu Cheng, Dacheng Zhang, Hexing Li and Guohua Liu*

Developments of magnetic nanoparticles (MNPs) for use as supports and explorations of their applications in aqueous catalysis represent an important branch of green chemistry as they enable environmentally friendly and sustainable catalytic processes. Besides significant merits to easily recover magnetic nanoparticles from reaction system, various strategies through surface modification, grafting and self-assembly offer a broad scope of approaches for constructing magnetically recoverable heterogeneous catalysts. In this review, we focus on the green catalytic processes and summarize recent advances in organic transformations catalyzed by magnetically recoverable catalysts (MRCs). This paper is divided into two main parts: The first part provides background information on the general preparations, modifications, and characterizations, where the modifications of various magnetic nanoparticles through the coating with silica, carbon, metal, or polymer were also presented. The second part provides a basic outline of aqueous catalysis based on water-only or water-and-organic solvent cosolvent system, in which numerous types of organic transformations are catalyzed by magnetically recoverable catalysts. Lastly, perspectives for further development of magnetically recoverable heterogeneous catalysts in aqueous catalysis are addressed.

1. Introduction

Classical heterogeneous catalysts with particle size typically on the micrometer scale are a kind of catalysts that are most widely used in industries. Their applications range from chemical manufacturing to energy harvesting to conversion and storage, and to environmental technology, covering more than 80% of industrial process.^{1,2} Especially, with the developments in nanoscience and nanotechnology, a wide variety of nanostructured catalysts or solid-supported nanostructured catalysts have been applied to various catalytic reactions. Such catalysts have been used because of high activity and high selectivity due to their small size (1–100 nm) and exposed active metallic or organometallic center. Recently, lots of these catalysts have worked for millions of turnovers, at high reaction rates, and with high selectivity. In some cases, many unattained novel properties can be found to contribute the superior catalytic performance compared with that of classical catalysts. These significant advantages are attributed to their nanosize effect; catalytic activity usually increases with decreasing size of nanoparticles. However, when the size of active site is reduced to nanoscale dimensions, the surface free energy is increased greatly. This effect promotes aggregation of the particles into small clusters and degrades the catalytic efficiency. Furthermore, isolation and recovery for heterogeneous catalysts become difficult as their size decreases

to nanoscale dimensions; in most cases, separation through conventional filtration may even become impossible. Thus, it is highly desirable to employ appropriate support materials and to develop highly efficiently recycling methods for catalysts.

Magnetic nanoparticles (MNPs), a type of alternative support or catalyst-supported material, have been recently explored extensively. They possess high thermal and mechanical stability and are amenable to large-scale production. Furthermore, their unique paramagnetic nature and inherent insolubility in most reaction solvents allow their simple and efficient separation from the reaction mixtures using an external magnetic field. These characteristics thus make them more sustainable. Furthermore, the minimal workup procedures required and the minimal amount of waste generated from their preparation adequately satisfy the requirements of the green chemistry principles. Furthermore, using an appropriate surface modification for magnetic nanoparticles may be done to prevent the aggregation of magnetic nanoparticles, leading to stable, finely dispersed active species. Because of these advantages, functionalized magnetic nanoparticles have found wide applications in various areas such as magnetic resonance imaging,^{3,4} biomedicine,^{5–8} and heterocatalysis.^{9–16} In particular, recent advances in magnetically recoverable catalysts (MRCs) have led to their wide use in oxidation,^{17–19} hydrogenation,^{20,21} coupling reaction,^{22–24} cycloaddition,^{25,26} acylation,^{27,28} photocatalysis,^{29–31} and so forth.

On the other hand, with the ultimate goal of solving environmental problems, the search for environmentally friendly

reaction media such as water and its cosolvents have gained high importance in the field of catalysis. Recently, catalytic reactions using green solvents in catalytic processes have contributed greatly to the number of applications in the industry. Water and its cosolvents have replaced organic solvents as the most convenient solvents in catalysis. They have many inherent advantages in terms of cost, availability, safety, and environmental impact. As noted in a review by Fokin³², water possesses many unique physical and chemical properties: a large temperature window in the liquid state, extensive hydrogen bonding, high heat capacity and large dielectric constant. More importantly, water can provide a notable improvement in reactivity, in many cases, enhancing reaction rate and affecting reaction selectivity. Since Diels–Alder reactions greatly accelerate in aqueous medium, water as reaction solvent for organic transformations has attracted much interest.^{33–35} With the rapid development in green chemistry, organic reactions in water and its cosolvents have become one of the most exciting research fields. The range of reactions have expanded to include C–C coupling reactions,^{36–38} click chemistry,^{39–43} rearrangement,^{44,45}

multicomponent reactions,^{46–50} bromination reactions,^{51,52} and oxidation and reduction.^{53–55} Several detailed reviews on these reactions have been published recently.^{32, 56–66}

In this review, we provide an overview of the applications of MRCs and their applications in aqueous medium. We start with the preparations and modifications of MNPs, and then discuss characterization by key methods such as X-ray diffraction (XRD), electron microscopy, and ferromagnetic resonance. Finally, we focus on organic transformations in aqueous medium catalyzed by MRCs. We elaborate the application of MRCs in aqueous catalysis according to the reaction solvent system. In the section for organic transformations in the water-only phase, we present metal catalysts, organometallic catalysts and organocatalysts supported onto MNPs. Organic transformations in water-and-organic solvents as cosolvent phase are discussed in a subsequent section. Finally, we discuss perspectives in future developments in this field.

Table 1 Typical methods for MNPs syntheses.

Synthetic method	Procedure	Solvent	Reaction period	Temperature	Size distribution	Shape control	Yield
Coprecipitation	Very simple, ambient condition	Water	Minutes	20–90 °C	Narrow	Poor	High/scalable
Microemulsion	Complicate, ambient condition	Cosolvent	Hours	20–50 °C	Narrow	Good	Low
Hydrothermal reaction	Simple, high pressure	Water-ethanol	Hours-days	200 °C	Very narrow	Very good	Medium
Thermal decomposition	Complicate, inert atmosphere	Organic	Hours-days	100–320 °C	Very narrow	Very good	High/scalable
Sol-gel reaction	Complicate, ambient condition	Organic	Days	60–400 °C	Very narrow	Good	Medium

2. Preparations, modifications and characterizations of MNPs

2.1 General preparations of MNPs:

Magnetic nanoparticles based on pure metals (such as Fe, Co, or Ni), metal oxides (such as Co_3O_4 , Fe_3O_4 , or $\gamma\text{-Fe}_2\text{O}_3$), or alloys (CoPt_3 , CoFe , or FePt), as well as spinel-type ferrites (MFe_2O_4 , where M is Fe, Co, Mn, Ni, or Cr), have been widely used in various research areas,^{67–69} such as biomedicine, magnetic storage media, and magnetic resonance imaging. Such applications are reviewed in various works.^{3,70–75} MNPs may be synthesized through several typical methods, including coprecipitation,^{76,77} microemulsion synthesis,^{78–80} hydrothermal synthesis,^{81,82} thermal decomposition,^{83,84} sol-gel,^{85–89} and others.^{90–95} Recently, these methods have been reviewed by Muller⁹⁶ and Schüth,⁷⁰ thus, details on the preparations of MNPs are not presented in this review. A general summary of such methods is presented in Table 1.

2.2 General modifications of MNPs:

An intrinsic disadvantage of MNPs is rapid aggregation to large cluster and consequent loss of unique properties associated with

catalytic reactions. Thus, MNPs are normally coated with specific organic or inorganic materials to prevent irreversible aggregation and to retain their nanoscale properties. In this review, we also summarize general methods for the modification of MNPs with silica, carbon, precious metal, or polymer (Table 2).

Table 2 Methods for MNPs modifications.

Method	Procedure	Temperature	Application
Silica coating	Simple	20–25 °C	Catalyst, drug delivery
Carbon coating	Complicated	20–400 °C	Catalyst
Metal coating	Simple	20–25 °C	Catalyst
Polymer coating	Complicated	20–80 °C	Catalyst, carrier

2.2.1 Silica coating of MNPs. Silica is the most common material for coating the surfaces of MNPs. Such coating is well-known for its ability to prevent magnetic aggregation in solution and its ability to improve chemical stability. Moreover, the surface of silica-coated MNPs is rich in silanol groups, which can react with various coupling agents for covalent attachment of functional groups. Especially, the sol-gel process, which relies on the well-known Stöber method,^{97–102} is a preferred method for coating of MNPs.

Typically, it form inorganosilicate or organosilicate coating-layer onto MNPs.

The inorganosilicate coating of MNPs is generally formed through *in situ* hydrolysis and condensation of silicon alkoxides (typically tetraethyl orthosilicate) in an alcohol/water mixture under basic conditions. Since the discovery in 1992,¹⁰³ highly ordered, mesoporous inorganosilicate materials have been the main choice for coating applications. Integration of mesoporous materials, magnetic response of MNPs and functionalized inorganosilicate shells have attracted increasing interest in MNPs with inorganosilicate coating because of their special physical and chemical properties such as large surface area, magnetic function, low toxicity, and chemically modifiable surfaces. These properties make them attractive for various applications, including drug delivery carriers, multimodal imaging agents, and water-treatment adsorbents and MRCs.^{104–111}

Organosilicate coatings of MNPs are conveniently constructed through the methods developed by Inagaki and Stein, as well as by Ozin group.^{112–114} A class of organo-inorganic nanocomposites known as periodic mesoporous organosilicas (PMOs) are built from bridged organosilane precursors (R'O)₃Si–R–Si(OR')₃ in the presence of a surfactant. In such coatings, organic groups (R) are an integral part of the mesoporous organosilica wall. In contrast to inorganosilicate coatings, PMO-type organosilicate coatings possess high lipophilicity, which is useful for drug delivery, adsorbents, and immobilization of catalysts. A highly versatile nanomaterial may formed by integrating the advantages of PMO materials and MNPs. For example, the groups of Qiao¹¹⁵ and Yu¹¹⁶ reported two kinds of magnetic, hollow PMO spheres that can be potentially applied in targeted delivery. Zhao group¹¹⁷ also prepared magnetic spherical cores partly coated with PMO-type single crystals that confer high specific surface area, good magnetic response, embedded functional groups, and cubic mesopore channels, which enable their use in various convenient applications.

2.2.2 Carbon coating of MNPs. Mesoporous carbon is another coating based on a main-group element that is used formagnetic nanoparticles. Several investigators have attempted to coat Fe₃O₄ spheres with glucose. The typical carbon layer is obtained by heating polymer-stabilized Fe₃O₄ nanoparticles at high temperature in an inert environment.^{118–121} The carbon layer can efficiently protect the Fe₃O₄ spheres from dissolving in acidic environments because its dense structure can inhibit penetration of hydrogen ions. Diao group¹²² demonstrated the construction of a magnetically separable Pd catalyst based on carbon-coated Fe₃O₄ nanoparticles, which exhibits good catalytic activity for Suzuki and Heck coupling reactions. Tsang group¹²³ also revealed that carbon-encapsulated magnetic nanoparticles in quasispherical carbon shells can be prepared on a large scale through a simple synthetic technique. In addition, the effect of carbon encapsulation based on the magnetic Ni-based nanoparticles was also involved in Amaratunga's report.¹²⁴

2.2.3 Metal coating of MNPs. Coating of MNPs with precious metals such as gold, platinum, or palladium^{125–128} leads to very useful, bimetallic magnetic nanoparticles. For example, magnetic nanoparticles coated with Au have distinct advantages over its counterpart based on a single-metal component.¹²⁹ In recent years, colloidal Au-coated magnetic nanoparticles have been the subject of strong interest in areas of materials science, biotechnology, and chemistry because of their function in molecular markers, diagnostic imaging, and catalysts.¹³⁰ Sun and coworkers¹³¹ demonstrated that dumbbell-like, Au-coated Fe₃O₄ nanoparticles are catalytically more active in H₂O₂ oxidations than either Au or Fe₃O₄ nanoparticles. Very recently, new and simple methods^{132–134} for the synthesis of Au-coated MNPs have been developed. These methods have expanded applications of MNPs coated with various precious metals.

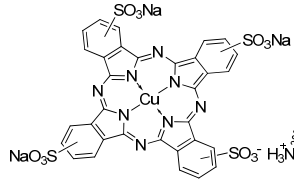
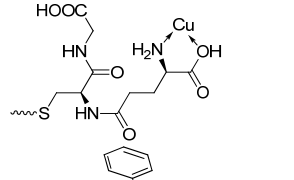
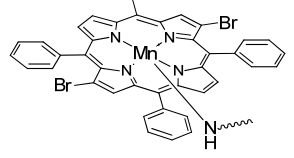
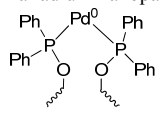
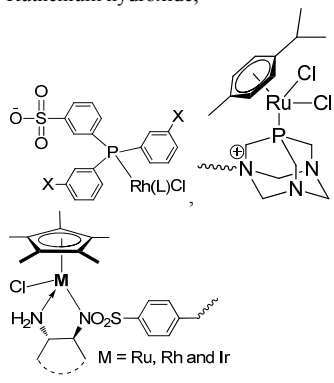
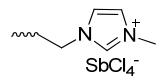
2.2.4 Polymer coating of MNPs. Coating of MNPs with polymers is another approach to stabilize MNPs. The typical method of surface-initiated atom transfer radical polymerization has been widely applied in coating of MNPs.^{135–138} Neoh and his coworkers¹³⁹ applied copper-mediated atom transfer radical polymerization to graft poly(poly(ethylene glycol)monomethacrylate) onto Fe₃O₄ nanoparticles. The grafted polymer chains are stable and enable modified MNPs to disperse well in aqueous solutions. Tatongroup¹⁴⁰ encapsulated magnetic γ -Fe₂O₃ nanoparticles with cross-linked polystyrene-*block*-polyacrylate micelle shells. Very recently, Paikgroup¹⁴¹ described polystyrenes end-functionalized with nitrilotriacetic acid as multifunctional nanocarriers for aqueous dispersions of CdSe, γ -Fe₂O₃, and Au nanoparticles.

2.3 General characterizations of MNPs:

Various techniques can be employed to characterize MNPs. XRD is often used to prove the crystalline structure and the phase purity of particles. The diffraction pattern can be used to quantify the proportion of iron oxide formed in the mixture by comparing the peak intensities in the experimental and reference diffractograms.¹⁴² It can also be used to calculate the crystal sizes through evaluation of the line broadening (in radians) and the corresponding Bragg angle. Scanning electron microscopy and transmission electron microscopy (TEM) are used to determine the size uniformity, shape of MNPs, shell thickness, and elemental composition of the core-shell structures. In addition, the hysteresis loop, which depicts the change in magnetization with the strength of an applied magnetic field, is a useful tool for evaluating the magnetic behavior of MNPs.⁷³ MNPs in the superparamagnetic state have much weaker magnetic dipole interactions and are therefore readily stabilized and dispersed in liquid media. Other techniques such as thermogravimetric analysis, Fourier transform infrared spectroscopy, X-ray photoelectron spectroscopy (XPS), and atomic force microscopy are often used to investigate the surface properties of stabilized and modified MNPs.⁹

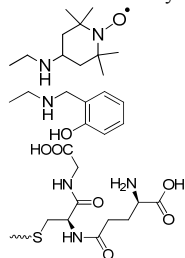
ARTICLE

Table 3 Classifications of catalytic species in a water-only phase

Types of catalyst	Catalyst	Organic transformation	Reference
Metal/Organometallic catalyst	$\gamma\text{-Fe}_2\text{O}_3$ or Fe_3O_4 ,	Condensation Reduction Knoevenagel-Michael-cyclization Oxidation	144–149
	Ag Silver nanoparticles	Reduction	150–154
	Au Gold nanoparticles	Reduction	155–164
	Copper nanoparticles or Cu(I) or Cu(II), 	Epoxidation and Oxidation Cycloaddition Oxidative polymerization Hydrolysis	165–172
	Cu 		
	Mn 	Oxidation	173–175
	Ni Nickel nanoparticles	Reduction	176–177
	Pd Palladium nanoparticles; Pd(II); 	Hydrogenation Suzuki–Miyaura cross-coupling Sonogashira coupling O-arylation O-allylation	178–181
	Pt Platinum nanoparticles	Hydrogenation Reduction	182–184
	Ruthenium hydroxide,		
Ru/Rh/Ir	 M = Ru, Rh and Ir	Hydration Hydrogenation Addition reaction Asymmetric transfer hydrogenation	185–192
Sb	 SbCl_4^-	Clauson-Kaas reaction	193
W	$\text{H}_3\text{PW}_{12}\text{O}_{40}$	Mannich-type reaction	194, 195

Organocatalyst

Dodecyl benzenesulfonic acid
Sulfuric acid
Sulfamic acid
Amino acids
 β -Cyclodextrin
Polyaniline (mPANI)
1-Azonia-4-azabicyclo[2.2.2]octane



Hydrolysis
Paal-Knorr reaction
Aza-Michael-type reaction
Coupling reaction
Multi-component condensation reaction
Knoevenagel condensation 196–212
Cyclocondensation
Asymmetric Adol reaction
Oxidation
Nucleophilic substitution reaction
S-Arylation

3. Application in aqueous catalysis

Aqueous catalysis is a well-known component of biological processes. Notably, a chemical catalysis in aqueous medium provides environmentally benign alternatives to current catalytic techniques in organic transformations. Sharpless and co-workers¹⁴³ define aqueous reactions as those in which insoluble reactant(s) are stirred in aqueous emulsions or suspensions without addition of any organic cosolvents through a catalytic process. However, in many cases, it is difficult to determine whether a reaction occurs in aqueous medium. Thus, as long as reaction mixture remains heterogeneous and overall process benefits the reaction rate or selectivity, the reaction is considered as an aqueous reaction in extensive definition. In many examples of such aqueous reactions, water-and-an organic cosolvent phase such as a lower alcohol, acetone, dimethyl formamide (DMF), and acetonitrile are employed in water, which it qualifies in an aqueous system. In this section, we discuss organic transformations catalyzed by MRCs classified according to the reaction solvents. These types are, namely, organic transformations in a water-only system (Table 3) and those in a cosolvent system of water-and-organic solvent (Table 5).

3.1 Organic transformations in a water-only phase

3.1.0 MNP-self-based MRCs: Magnetic nanoparticles and analogs coated/modified with metal or organometallics or organic molecules have a wide range of applications in water-only catalytic systems. In such systems, the magnetic core provides a magnetic function and the functionalized shell participates in catalysis. It is worth mentioning that, in many cases, magnetic nanoparticles (such as Fe_3O_4 and $\gamma\text{-Fe}_2\text{O}_3$) not only function as a magnetic core. The Lewis acid nature of iron sites as also catalyzes a number of organic reactions. Therefore, magnetic nanoparticles themselves can function as MRCs for various catalytic reactions in a water-only phase.

An example is reported by Karami group.¹⁴⁴ They used iron in Fe_3O_4 nanoparticles as Lewis acids to activate the carbonyl group in aldehydes for nucleophilic attack. They found that the nanoparticles could catalyze the condensation reaction of aryl aldehydes and 1,3-cyclohexanediones in water to form high

yields of 9-aryl-substituted 1,8-dioxo-octahydroxanthenes (Fig. 1). The attractive features of this protocol are the simple workup procedure, very short reaction time, and high reusability of the catalyst. These features constitute an economic advantage for organic transformation.

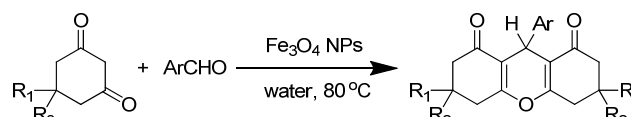


Fig.1 The syntheses of 1,8-dioxo-octahydroxanthenes catalyzed by Fe_3O_4 nanoparticles (NPs).

Similarly, Dash group¹⁴⁵ reported a reduction reaction in water using Fe_3O_4 MNPs as catalyst. Here, azides were converted to the corresponding amines by using hydrazine hydrate as the hydrogen source. This reaction is suitable for a broad range of organic azides and has excellent yields. Furthermore, The Fe_3O_4 MNPs could be magnetically recovered and efficiently reused for 10 catalytic cycles without significant loss of catalytic efficiency. These results indicate its potential industrial applications because of the simple, green catalytic process.

Furthermore, the use of iron magnetic nanoparticles could be extended to multiple-component organic transformations. Safari group¹⁴⁶ synthesized 2-amino-4H-chromene *via* one-pot three-component coupling of aldehyde, malononitrile, and resorcinol in water using Fe_3O_4 MNPs as catalyst at room temperature (Fig.2). The Fe_3O_4 MNPs exhibited excellent catalytic performance within short reaction time in the reaction of up to 18 tested aldehydes, leading to high yields. The small size (18 nm) of the Fe_3O_4 MNPs enabled them to function as nanoreactors. Moreover, the Fe_3O_4 MNPs could be easily separated by using magnetic devices and could be reused in the catalytic reaction without any apparent loss of activity.

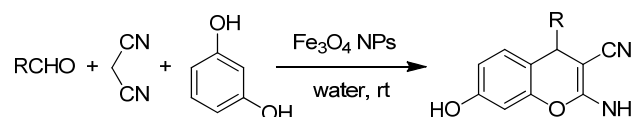


Fig.2 The syntheses of 2-amino-4H-chromenes catalyzed by Fe_3O_4 nanoparticles (NPs).

Very recently, Rostamia group¹⁴⁷ reported a three-component Knoevenagel–Michael cyclization coupling reaction. In their work, they employed water-dispersible, magnetic γ -Fe₂O₃ MNPs (H₂O-DMNPs) as a MRC to construct a variety of annulated tetrahydro-4*H*-chromenes and polyhydroquinolines in high yields under mild conditions. The MRC could be reused in five consecutive runs. Meanwhile, the similar γ -Fe₂O₃ MNPs supported on hydroxyapatite were also explored by Jayaram group.¹⁴⁸ In their study, γ -Fe₂O₃ MNPs enabled three-component one-pot synthesis of disubstituted 1,2,3-triazoles from terminal alkynes and organic azide that *in situ* generated in water. Their present protocol is applicable to a broad range of substrates that are combined, such as aromatic/aliphatic alkynes, and halides containing aromatic and aliphatic groups (up to 36 tested substrates). Also, the catalyst could be reused for up to five consecutive cycles without loss of catalytic activity.

An interesting work was reported by Rajabi and coworkers.¹⁴⁹ In their work, they utilized mesoporous SBA-15 material as a support and prepared SBA-15-supported Fe₃O₄ MNPs that was applied in the oxidation of styrene derivatives in water. It is worth mentioning that the catalyst could be used at low loadings (0.5 mol%) to convert styrene derivatives to aldehydes with >90% yields. The reaction is carried out under mild conditions by using hydrogen peroxide, a green oxidant. The supported catalyst could be easily recovered and reused without any loss of activity. Their study significantly enriched the use of MRC in aqueous oxidation chemistry.

3.1.1 Ag-functionalized MRCs: Silver, a traditional catalyst that is used most widely, has gained much attention. It has been applied in the reduction of 4-nitrophenol (4-NP) in the presence of NaBH₄ in water. A general model for its catalytic action could be postulated as follows. First, borohydride ions reversibly transfer a surface-hydrogen species to the surface of Ag. Concomitantly 4-NP is adsorbed. The rate-determining step is the reduction of 4-NP by the surface hydrogen species. Finally, reduction products are obtained, completing the catalytic cycle. So far, several magnetic materials, including bare γ -Fe₂O₃ nanospheres, silica-coated γ -Fe₂O₃ nanoparticles, and carbon-coated γ -Fe₂O₃, have been used as supports for the preparations of Ag-functionalized MRCs.

An earlier work was reported by Shin and coworkers.¹⁵⁰ In their work, they directly deposited Ag nanoparticles onto the surface of γ -Fe₂O₃ nanoparticles by *in situ* reduction in an ethanolic AgNO₃ and butylamine system to fabricate Ag-deposited γ -Fe₂O₃ nanoparticles. The nanoparticles were suitable for catalytic reduction of 4-NP in the presence of the NaBH₄, exhibiting good catalytic activity in water. Furthermore, the nanoparticles could be readily recovered from the solution phase by the use of a small magnet. An improved preparation method, which was performed by Jiang and co-workers,¹⁵¹ employed a sonochemical approach for *in situ* reduction of Ag ion to Ag in the substitution of chemical reductants. This method provides a green, efficient process for preparing Ag-functionalized MRCs.

An improved strategy was reported by Li and co-workers.¹⁵² In contrast to the method of Shin group¹⁵⁰, they utilized a

strategy of silica coating to form silica-coated Ag-functionalized MRC (Fe₃O₄@SiO₂-Ag) with core-shell structure. The obvious benefit of the strategy is the *in situ* reduction of Ag ion to Ag through the aid of polyvinylpyrrolidone (PVP, a reductant and stabilizer) during the preparation. As a result, small Ag nanoparticles highly dispersed onto the silica layers could be steadily obtained. This strategy effectively prevented the aggregating of Ag nanoparticles on the silica surface. The Fe₃O₄@SiO₂-Ag nanoparticles also showed high performance in the catalytic reduction of 4-NP. They could be easily recycled by applying an external magnetic field without loss of catalytic activity within 15 cycles of reuse.

Meanwhile, a polystyrene (PS)-coated Ag-functionalized MRC (Fe₃O₄@PS@PAMAM-Ag) was also prepared by Yang and coworkers.¹⁵³ Their approach used PS as a coating and carboxylic groups of polyamidoamine (PAMAM) dendrimers as reductant and stabilizer to form Fe₃O₄@PS@PAMAM-Ag nanoparticles. Similar to the silica-coated Fe₃O₄@SiO₂-Ag nanoparticles prepared by Li group¹⁵², this magnetic catalyst also comprises highly dispersed, nanosized Ag nanoparticles that could be steadily embedded in PAMAM dendrimer shells. The catalyst also showed high performance in the reduction of 4-NP in the presence of the NaBH₄ in water. In contrast to the silica-coated Fe₃O₄@SiO₂-Ag nanoparticles¹⁵², the catalyst had relatively low recyclability (6 times *vs* 15 times) because the PS-coated layers have lower chemical stability compared with that of SiO₂-coated layers. Very recently, Diao and coworkers¹⁵⁴ reported a carbon-coated Ag-functionalized MRC (Fe₃O₄@C-Ag) with similar core-shell structure. The preparation strategy used in their study is a carbonization in which a thin layer of carbon is coated by *in situ* carbonization of glucose under hydrothermal conditions to form the core-shell magnetic Fe₃O₄@C-Ag. The nanosized Ag nanoparticles were also highly dispersed and had high catalytic activity in the reduction of 4-NP in the presence of NaBH₄ in water.

3.1.2 Au-functionalized MRCs: Similar to Ag-functionalized MRCs, Au nanoparticles on magnetic materials could be also used to construct Au-functionalized MRCs. Peng and co-workers¹⁵⁵ reported Au-functionalized MRC through a co-precipitation of Fe₃O₄ and AuCl₄ at room temperature. In their work, they utilized oleylamine as a reductant to *in situ* form Au-coated magnetic nanoparticles. The as-prepared catalyst showed good catalytic activity for 4-NP reduction in the presence of NaBH₄ in water. Furthermore, Chen and colleagues¹⁵⁶ reported SiO₂-coated Au-functionalized MRC (Fe₃O₄@SiO₂-Au). In contrast to those in the co-precipitation method, Au nanoparticles in this process were formed by *in situ* reduction of trivalent Au ion by bivalent Sn ion in solution, and were then linked to the surface of SiO₂-coated Fe₃O₄@SiO₂ precursors. Fe₃O₄@SiO₂-Au showed the high catalytic performance in the reduction of 4-NP in the presence of the NaBH₄ in water. After the reaction, the catalyst could be separated and subsequently used for nine consecutive cycles. Similarly, both groups of Yang group¹⁵⁷ and Zhu group¹⁵⁸ also reported the preparation of coated-type Fe₃O₄@SiO₂-Au. Yang

group synthesized hierarchical magnetite/silica/poly(ethylene glycol dimethacrylate-*co*-4-vinylpyridine) trilayer microspheres and used them as stabilizers for gold metallic nanocolloids. Zhu group constructed multifunctional magnetic composite microspheres by *in situ* growth of Au nanoparticles in multilayer polyelectrolyte films. Magnetic microspheres prepared by both groups showed good catalytic performance in the reduction of 4-NP in water.

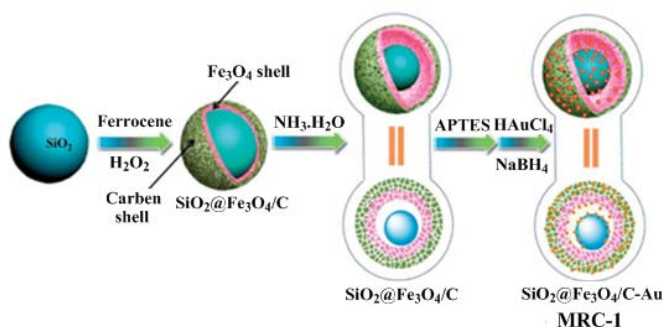


Fig.3 The schematic preparation of MRC-1.

Also, Au nanoparticles can also be immobilized within the inside surface of yolk-like structural magnetic material. Cai group¹⁵⁹ reported Au nanoparticles based on the double-shelled, yolk-like structural Au-functionalized MRC-1, which was used for the reduction of 4-NP in the presence of NaBH₄ in water. As shown in Fig.3, SiO₂ nanoparticles were coated with a double-layered shell of Fe₃O₄ and carbon *via* a hydrothermal approach. The nanoparticles were etched in aqueous ammonia to obtain yolk-like, double-shelled microspheres, which were used for immobilization of the gold catalyst. The main benefit of this preparation strategy is its capability to form numerous gold nanoparticles (average size of 2 nm) within the interior cavity and the mesoporous shell. Evidently, the numerous, nanosized catalytic active sites led to the high catalytic performance of the microspheres in 4-NP reduction in the presence of NaBH₄ in water. In particular, the outer carbon layer of the yolk-like structure not only protects the Fe₃O₄ layer from harsh conditions of the external environment but also provides additional adsorption sites for Au nanoparticles in the interior. These characteristics enable the recycling of the catalyst for at least nine cycles, demonstrating its magnetically separable feature and good recyclability. Very recently, Chen group¹⁶⁰ developed another Au-functionalized MRC through immobilization of Au nanoparticles onto graphene oxide. The as-prepared catalyst had good recyclability and stability because it was synthesized by growth of Au nanoparticles from tiny Au seeds. The work of Chen group is very similar to that of Gupta group.¹⁶¹

An interesting work carried out by Yin and coworkers.¹⁶² Here, the Au-functionalized MRC-2 (Fe₃O₄/SiO₂/p-NIPAM/SiO₂-Au) was prepared by hierarchical assembly of silica colloids using nanosilver as template. Fig.4 outlines the synthetic procedure for MRC-2. First, SiO₂-coated Fe₃O₄ nanoparticles were functionalized with [3-

(methacryloyloxy)propyl]trimethoxysilane that had been copolymerized with *N*-isopropyl acrylamide and with *N,N'*-methylenebisacrylamide (cross-linker). After the as-prepared magnetic support in AgNO₃ solution was allowed to swell and reduced with NaBH₄, the Ag nanoparticles were obtained. An additional sol-gel process was performed to obtain satellite silica by using nanosilver as templates that stabilized Au nanoparticles. The main advantage of this Au-functionalized MRC is its large surface area. MRC-2 showed high activity in the reduction of 4-NP in the presence of NaBH₄ in water. The catalyst could be quickly separated from solution by the use of an external magnet and could be reused for 10 times without obvious decrease in its catalytic performance.

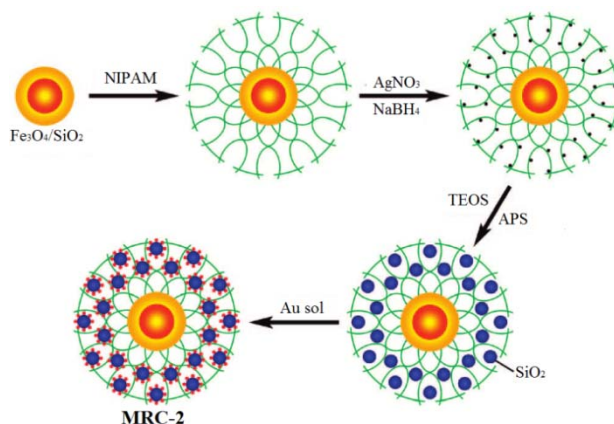


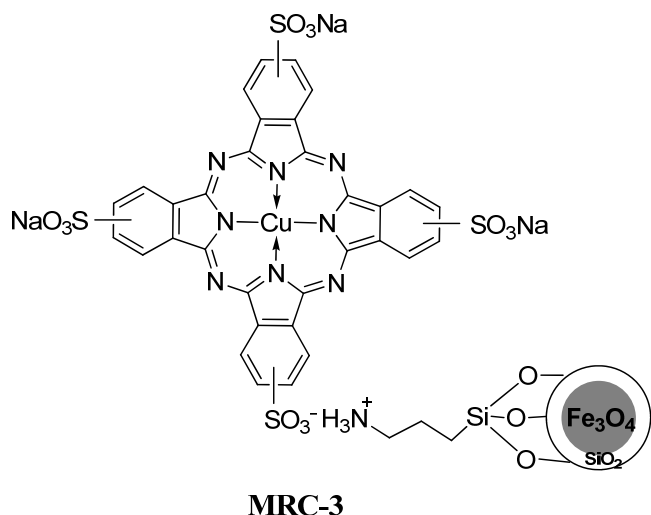
Fig.4 The schematic preparation of MRC-2.

Beside the application in the reduction of 4-nitrophenol in water, Au-functionalized MRCs are also applied in the reduction of potassium ferricyanide. Sun and coworkers¹⁶³ described a facile synthetic route to fabricate gold nanostars with Fe₃O₄ cores under mild reaction conditions. These Au-functionalized nanostars were used as MRC for the reduction of potassium ferricyanide in the presence of NaBH₄ at room temperature. This reaction was carried out in a quartz cuvette and monitored by UV-visible spectroscopy. The study showed that the MRC exhibited good performance in the reduction of potassium ferricyanide. It did not lose its catalytic activity in six successive reactions. Also, it could be applied in the reduction of 4-NP in the presence of NaBH₄ in water, which is similar to apolyethyleneimine-coated Au-functionalized MRC reported by Ma group.¹⁶⁴

3.1.3 Cu-functionalized MRCs: Generally, copper ion and its complexes have been extensively used to catalyze various oxidation, cycloaddition, and coupling reactions. In this case, Cu-functionalized MRCs are mainly used in oxidation, oxidative polymerization, and azide-alkyne cycloaddition.

In oxidation reaction, a representative Cu-functionalized MRC was reported by Rezaeifard and coworkers.¹⁶⁵ In their work, they immobilized Cu(II) phthalocyanine-tetrasulfonic acid tetrasodium complex (CuPcS) on silica-coated magnetic nanoparticles through ion-pair strategy to form Cu-functionalized MRC-3 (Fig. 5). This catalyst showed excellent

selectivity in the epoxidation of olefins and the oxidation of saturated hydrocarbons to the related ketones using tetra-*n*-butylammonium peroxomonosulfate as oxidant. The advantages of this reaction are that it does not require surfactants, additives, toxic reagents or solvents; it does not produce by-products; and it does not necessitate laborious purification. Also, **MRC-3** could be applied to the selective oxidation of sulfides to the sulfones in a water-only phase and to oxidation of sulfoxides in a water-ethanol phase. Although the anionic CuPcS complex is anchored electrostatically on silica-coated magnetic nanoparticles, the **MRC-3** could be recovered efficiently for at least seven times without obvious decrease in its catalytic performance in the oxidation of different kinds of substrates.



MRC-3

Fig. 5 The structure of **MRC-3**.

Most Cu-functionalized MRCs are applied in azide-alkyne cycloaddition reactions in water. The first example of such MRCs was reported by Moores, Li and coworkers.¹⁶⁶ They developed novel bimetallic copper-iron nanoparticles obtained

through *in situ* reduction of bivalent Cu ion to univalent Cu ion by the metal iron core of MNPs. The benefits of this system arise from the three-fold role of the iron core, namely, magnetic recoverability, reductant for formation of the active species univalent Cu ion, and support to prevent univalent Cu ion liberation. The bimetallic copper-iron nanoparticles exhibited high activity in azide-alkyne cycloaddition in water. The catalyst enabled production of a diverse range of triazoles, in which primary and secondary aliphatic, and traditional benzylic azides were expensively used to couple with aliphatic and aromatic alkynes (including alcohol-substituted alkynes) to generate triazoles. Especially, the reaction is very economical as it does not require reductants or ligands.

A more detailed exploration of azide-alkyne cycloaddition in water was reported by Varma group.¹⁶⁷ In their work, they reported another Cu-functionalized **MRC-4** and its application in Huisgen 1,3-dipolar cycloadditions (Fig. 6). The innovative strategy used in the synthesis is that glutathione was directly anchored to Fe₃O₄ surfaces through the use of the highly reactive thiol-functionality in the middle of glutathione, followed by the complexation of Cu ion to form **MRC-4**. This strategy keeps active sites free for highly efficient catalysis not only in the traditional two-component azide-alkyne cycloaddition, but also in three-component one-pot reaction of alkyl halides, aromatic alkynes, and sodium azide. Results of the study indicate that the triazole was formed regioselectively without production of the 1,5-regioisomer. In most tested cases, the reactions proceeded smoothly and finished within 10 min with excellent yields. **MRC-4** could be reused at least three times without obvious decrease in activity. A contribution is that glutathione itself onto Fe₃O₄ nanoparticles can serve as organocatalysts for the Paal-Knorr reaction and homocoupling of boronic acids. Another contribution is that a variety of Pd- or Ru-functionalized MRCs could also be constructed conveniently discussed below.

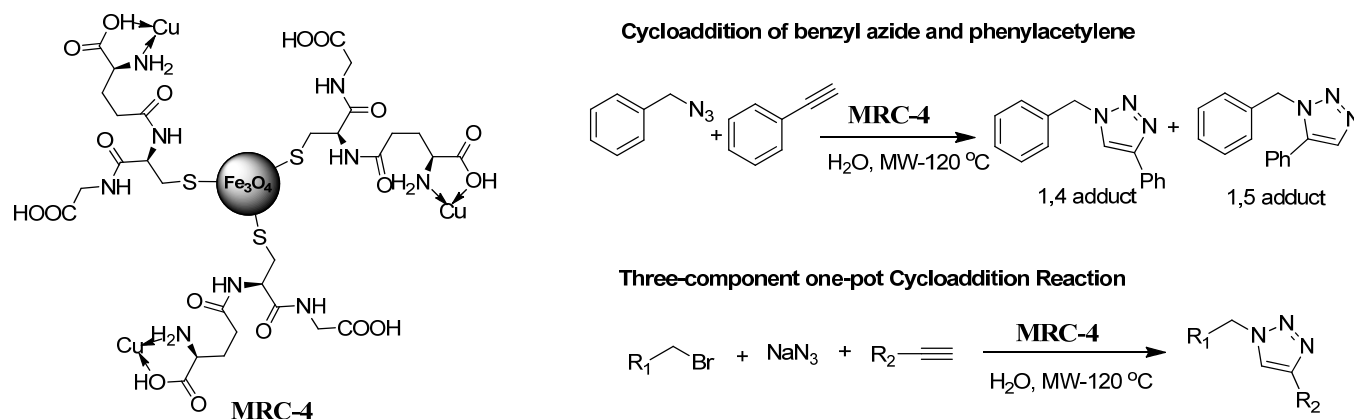


Fig. 6 The structure of **MRC-4** and its catalytic reactions.

Very recently, two similar Cu-functionalized **MRC-5** and **MRC-6** (Fig. 7) were reported by Xiong and Cai.¹⁶⁸ They also directly modified Fe₃O₄ nanoparticles with (3-

aminopropyl)trimethoxysilane and [3-(2-aminoethylamino)propyl]trimethoxysilane *via* a postgrafting method followed by the complexations with CuBr to generate

MRC-5 and **MRC-6**, respectively. In the one-pot three-component reaction of benzyl chloride, phenylacetylene, and sodium azide to 1,2,3-triazoles, the azide–alkynes cycloaddition reactions in water using PEG-400 as phase transfer catalyst under microwave irradiation afforded the target products with good yields, in which **MRC-5** was a more effective catalyst than **MRC-6**. Furthermore, they extended the use of **MRC-5** to various halides and terminal alkynes and demonstrated its versatility. As stated in the presented study, microwave irradiation could distinctly shorten the reaction time and simultaneously enhance the yields in comparison with conventional protocols. An important contribution of the one-pot three-component azide–alkyne cycloaddition is that synthesis of 1,2,3-triazole derivatives in water could be scaled up to a multi-gram production, which will be edged in industrial application.

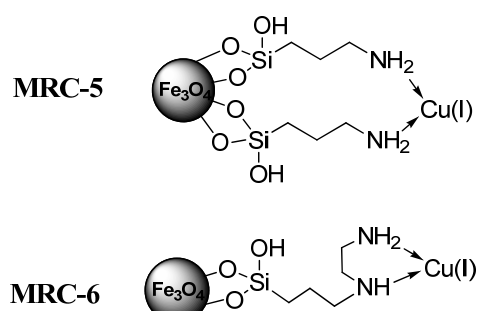


Fig. 7 The structures of **MRC-5** and **MRC-6**.

Among the Cu-functionalized MRCs, a few examples were used in studies on oxidative polymerization. Shentu and coworkers¹⁶⁹ performed direct grafting of poly(amindoamine) onto magnetic Fe_3O_4 nanoparticles followed by coordination with bivalent Cu ion to form a Cu-functionalized MRC (Cu/Mag-PAMAM). This catalyst catalyzed the oxidative polymerization of 2,6-dimethylphenol in water, yielding poly(2,6-dimethyl-1,4-phenylene oxide) with excellent C–O/C–C selectivity. Moreover, the magnetic catalyst were recovered and subsequently used for three consecutive cycles, the recovery ratio of the catalyst reached ~95% and the yield of the target product maintained a relatively high value.

Besides the application of Fe_3O_4 nanoparticle as magnetic support for preparation of Cu-functionalized MRCs, CuFe_2O_4 nanoparticles and cobalt ferrite magnetic nanoparticles could also be used in the synthesis of Cu-functionalized MRCs. A typical example of such nanoparticles is magnetically recoverable CuFe_2O_4 nanoparticles reported by Nageswar group.¹⁷⁰ They were applied in azide–alkyne cycloaddition to synthesize 1,2,3-triazoles. This Cu-functionalized MRC showed highly efficient catalytic activity and good recyclability. The advantage is that CuFe_2O_4 nanoparticles are commercially available, and thus have potential applications in industries. In the one-pot catalytic preparation of 1,2,3-triazoles, the benzyl halides are initially substituted with sodium azide through *in situ* formation of benzyl azides, which could be smoothly reacted with alkynes in water. This method is simple, facile and

applicable to a wide range of substrates with high functional group tolerance. The CuFe_2O_4 nanoparticles could also be used to construct 1,4-diaryl-1,2,3-triazoles from boronic acids, sodium azide, and acetylenes through the one-pot three-component azide–alkyne cycloaddition reported by Sreedhar and coworkers.¹⁷¹

Interestingly, Kaya group¹⁷² reported a silica-coated CoFe_2O_4 -based Cu-functionalized MRC (CuNPs@SCF) and its application in the hydrolysis of ammoniaborane (NH_3BH_3). Importantly, copper nanoparticles were reproducibly supported on SiO_2 -coated CoFe_2O_4 through wet-impregnation of bivalent Cu ions on SiO_2 -coated CoFe_2O_4 followed by *in situ* reduction on the surface of the magnetic support during hydrolysis of NH_3BH_3 . The MRC were highly active in the hydrolysis of ammonia-borane, providing an initial turnover frequency higher than that achieved with general homogeneous and heterogeneous catalysts employed in this reaction. In particular, this characteristics and high recyclability (10 cycles) make it more attractive as one of the most promising solid hydrogen carriers because of its high gravimetric hydrogen storage capacity and low molecular weight.

3.1.4 Mn-functionalized MRCs: Manganese is a well-known catalyst in oxidation reactions. In fact, considerable effort has been devoted to the study of porphyrin complexes, which are common biorelevant catalysts. In this case, only two Mn-functionalized MRCs were reported. Rezaeifard and coworkers reported¹⁷³ a SiO_2 -coated Mn-functionalized **MRC-7** (Fig. 8), and applied it to the selective oxidation of hydrocarbons and sulfides in water. Similar to the SiO_2 -coated method followed by a postgrafting approach, **MRC-7** was obtained through the coordinative anchoring of the manganese-porphyrin complex on silica-coated magnetic nanoparticles using an amine as a linker. **MRC-7** exhibited high catalytic activity in the oxidation of olefins and saturated hydrocarbons with tetra-*n*-butylammonium peroxomonosulfate in aqueous solution, strongly similar to a previous report on **MRC-3**¹⁶⁵. The catalyst showed enhanced efficiency and high selectivity, even at low Mn-loading in the catalytic process. Similarly, sulfides could also be converted selectively into sulfones in water-only phase, and to sulfoxides in water-ethanol phase. The experimental results showed that **MRC-7** could be recovered efficiently and reused at least seven times in the oxidation of various substrates with little decrement of the yield.

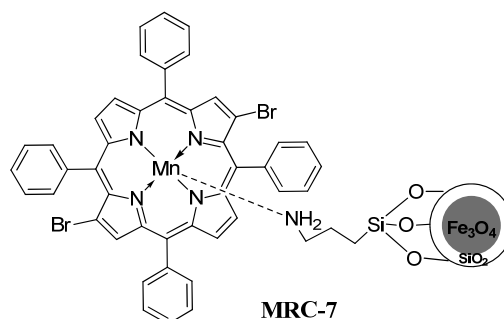
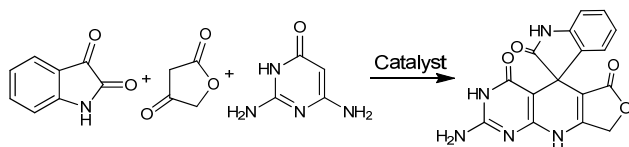


Fig. 8 The structure of **MRC-7**.

Another example of Mn-functionalized MRC is MnFe_2O_4 nanoparticles reported by Ghahremanzadeh and coworkers.^{174,175} They applied it to one-pot three-component synthesis of spiro-furo-pyrido-pyrimidine-indolines. As shown in table 4, the three-component reaction of isatin, tetrone acid, and 2,6-diaminopyrimidin-4(3H)-one completed in a shorter time and afforded enhanced yields in comparison with those with the other nanoparticles, including magnetic CuFe_2O_4 and Fe_3O_4 nanoparticles. In addition, this highly recyclable MnFe_2O_4 -based MRC could be used for the synthesis of several spirooxindoles with a good recyclability.

Table 4 A comparison of the three-component catalytic reaction.^a



Entry	Catalyst	Time (h)	Yield ^b (%)
1	Nano CuFe_2O_4	1	74
2	Nano MnFe_2O_4	1	82
3	Nano Fe_3O_4	1	60
4	Nano ZnO	5	>50
5	Nano MgO	5	52
6	Nano TiO_2	5	>50
7	Nano SnO_2	5	53

^aReaction conditions: isatin (1.0 mmol), tetrone acid (1.0 mmol), 2,6-diaminopyrimidin-4(3H)-one (1.0 mmol), H_2O (5 mL), 90°C , catalyst (10 mol %). ^b Isolated yields.

3.1.5 Ni-functionalized MRCs: Ni nanoparticles are important magnetic materials. In this case, there are only a few studies on the use of Ni-functionalized MRCs in a water-only phase, mainly focusing on hydrogenation of nitrobenzene. Shen group¹⁷⁶ utilized an *in situ* reduction approach to prepare a series of Ni-functionalized MRCs (magnetic Ni nanocomposites based on reduced graphene oxide(GO/Ni)) with various morphologies. The size of Ni nanoparticles on the graphene oxide sheets could be tuned from <5 nm to several tens of nanometers. Typical GO/Ni nanocomposites were prepared by addition of NiCl_2 to a stable colloidal dispersion of graphene oxide followed by reduction with hydrazine hydrate. Catalytic reduction of 4-NP in the presence of NaBH_4 in water could be markedly enhanced because of the peculiar electronic structure of GO and the prevention of Ni nanoparticle aggregation. Magnetic studies revealed that the GO/Ni nanocomposites, including nanocomposites with 2–4 nm Ni nanoparticles, displayed room-temperature ferromagnetic behavior. They could be easily separated from the reaction system by the use of a magnet.

Another Ni-functionalized MRC (cobalt–nickel alloy nanoparticles) was reported by Mandal group.¹⁷⁷ In their work, they prepared chainlike cobalt–nickel (CoNi) alloy nanoparticles through a wet chemical reduction method in a nonpolar solvent. Here, thermoresponsive poly(vinyl methyl ether) was used as a self-assembly reagent and hydrazine was used as a reduction reagent. Interestingly, the compositions of nanoalloys could be easily tuned by varying the initial molar

ratios of the precursors Co and Ni. This characteristic shows the soft ferromagnetic behavior, which is utilized in magnetic recovery. Similar to its parent Co and Ni nanoparticles, Ni-functionalized MRC exhibited good activity in the redox reaction of $\text{K}_3[\text{Fe}(\text{CN})_6]$ in the presence of $\text{Na}_2\text{S}_2\text{O}_3$ and in the reduction of 4-NP in the presence of NaBH_4 in water. Moreover, the catalyst could easily be recovered from the reaction mixture by use of a bar magnet and could be efficiently reused at least eight times without further purification.

3.1.6 Pd-functionalized MRCs: Pd nanoparticles are well-known catalysts for the formation of C–C bonds. Pd-catalyzed Heck, Suzuki, and Sonogashira coupling reactions were investigated extensively both theoretically and practically. Although there are many works on Pd-functionalized MRCs in aqueous medium (that will be discussed in a cosolvent phase of water-and-organic solvent below), studies on reactions in a water-only phase mainly involve hydrogenation, Suzuki–Miyaura, Sonogashira, and O-arylation/allylation of phenols.

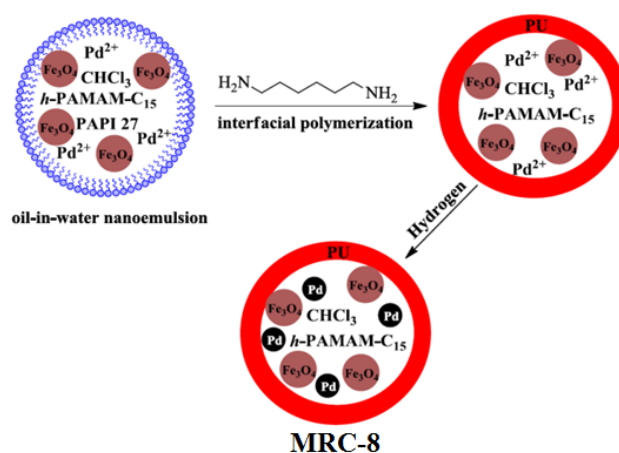


Fig.9 The schematic preparation of MRC-8.

In hydrogenation reaction, a representative Pt-functionalized MRC-8 was reported by Abu-Reziq and coworkers (Fig. 9).¹⁷⁸ In this process, they utilized a co-encapsulation strategy *via* a typical oil-in-water nanoemulsion, in which palladium nanoparticles are stabilized by hyperbranched polyamidoamine(*h*-PAMAM- C_{15}) with hydrophobic magnetite nanoparticles in polyurea nanospheres. Synthesis of polyurea nanospheres is based on nanoemulsification of chloroform containing magnetic nanoparticles and palladium acetate in water using suitable surfactants or dispersants. The chloroform nanodroplets are subsequently confined in a polyurea shell formed by interfacial polycondensation between isocyanate and amine monomers. The palladium acetate was reduced with hydrogen to create palladium nanoparticles dispersed in the core of the polyurea nanocapsules to form Pt-functionalized MRC-8. MRC-8 produced excellent yields in the reduction of aromatic alkenes in water under 200 psi H_2 pressure at room temperature. The contribution described here offers a novel method to construct nanoreactor-like MRC-8. Furthermore, MRC-8 was easily separated from the reaction mixture by the use of an external magnetic field and was efficiently reused for

four cycles without loss of its reactivity in the hydrogenation of styrene.

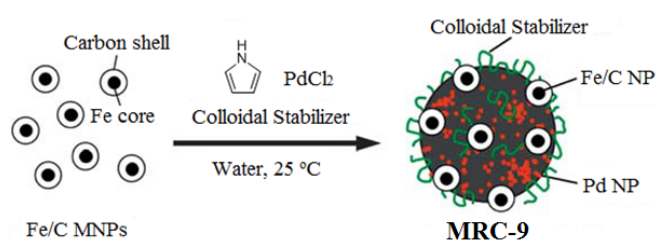


Fig.10 The schematic preparation of **MRC-9**.

In Suzuki–Miyaura cross-coupling, Fujii group¹⁷⁹ performed a single-step polymerization method to one-step synthesize a Pt-functionalized **MRC-9** (Fe–PPy–Pd ternary nanocomposite microspheres). By taking use of the inner magnetic attraction of the carbon-coated MNPs, they obtained poly-(4-ammonium styrene sulfonic acid) by *in situ* oxidative polymerization of pyrrole using PdCl₂ as oxidant. This polymer functioned as colloidal stabilizer congregating the carbon-coated MNPs and formed ternary magnetic nanocomposite microspheres (Fig.10). The significant advantage of this approach is that one-step synthesis takes place in aqueous media, which is suitable for industrial-scale production. The magnetic microspheres exhibited high catalytic activity in Suzuki–Miyaura cross-coupling of *p*-bromoacetophenone with *p*-methylphenylboronic acid in water using K₂CO₃ as a base. Furthermore, **MRC-9** was recovered from the dispersion medium by using a magnetic bar (up to 100% recovery), and was reused for four successive runs of the coupling reaction under the same conditions without any decrease in its yield.

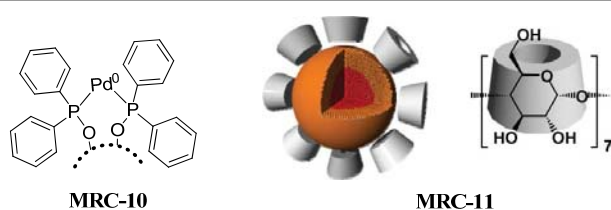


Fig. 11 The structures of **MRCs**.

In contrast to the one-step synthesis of Pd-functionalized **MRC-9** by Fujii group, a multistep procedure was developed by Zolfigol group¹⁸⁰ to prepare another Pd-functionalized **MRC-10**. This catalyst was applied to Sonogashira coupling and O-arylation of phenols. As shown in Fig.11, they used SiO₂-coated Fe₃O₄ nanoparticles in the immobilization of diphenylphosphine on the surface of SiO₂-coated MNPs followed by the coordination with PdCl₂, forming Pd-functionalized **MRC-10**. Because of the multistep procedure, **MRC-10** possessed highly dispersed, small nanoparticles with narrow size distribution relative to that of the catalyst prepared by Fujii group. **MRC-10** had high catalytic activity and extensive substrate scope in O-arylation of phenols with aryl halides; it included the less-activated aryl halides. It also showed the same properties in Sonogashira coupling under mild

conditions in water. Its high efficiency, wide applicability, and simplicity led to a highly efficient, clean and recyclable reaction, increasing its use in organic transformations.

In addition, Varma group¹⁸¹ also reported another Pd-functionalized MRC and applied it to O-allylation of phenols. In the synthesis, using dopamine as a robust anchor, Fe₃O₄ nanoparticles in aqueous suspension were sonicated to form dopamine-functionalized Fe₃O₄ nanoparticles. Coordination of dopamine-functionalized Fe₃O₄ nanoparticles with PdCl₂ afforded Pd-functionalized MRC. The spherical morphology of the catalyst and its relatively narrow size distribution (13–38 nm) led to its high catalytic activity in the O-allylation of phenols with allylic acetates in water under ambient conditions.

3.1.7 Pt-functionalized MRCs: Similar to Pd-functionalized MRC, a few Pt-functionalized MRCs are also applied in reduction and hydrogenation reactions. Yamashita group¹⁸² prepared a Pd-functionalized **MRC-11** (Fig. 11) through thermal decomposition of iron carbonyl (Fe(CO)₅) followed by reduction of platinum acetylacetonate (Pt(acac)₂) in the presence of oleic acid and oleylamine. Pt atoms are preferentially located in the shell region, whereas Fe atoms are preferentially located in the core region. Fe–Pt nanoparticles with an average diameter of 2.5 nm that had been capped with γ -cyclodextrin were successfully applied to hydrogenation of 4-NP in water. **MRC-11** exhibited enhanced catalytic efficiency in organic transformation in water relative to that in organic solvents. **MRC-11** could be easily recovered from water by applying an external magnet. It also preferred allyl alcohol over the sterically hindered 3-cyclohexene-1-methanol in competitive hydrogenation because of the molecular recognition imposed by the surface-attached γ -cyclodextrin.

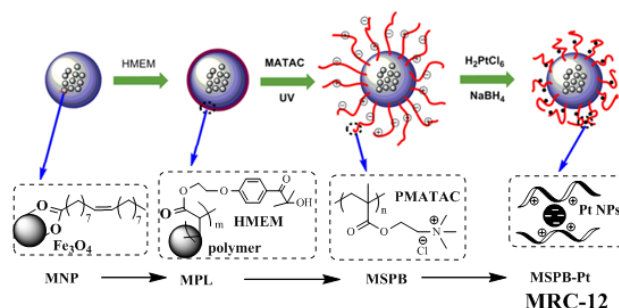


Fig.12 The schematic preparation of **MRC-12**.

Guo and coworkers¹⁸³ also reported a similar Pt-functionalized **MRC-12**, in which Pt nanoparticles with an average size of 3.5 nm were immobilized on magnetic spherical polyelectrolyte brushes (MSPBs). As shown in Fig. 12, MNPs were coated with polystyrene and a photoinitiator, (2-[*p*-(2-hydroxy-2-methylpropiophenone)]-ethylene glycol methacrylate. Afterward, photoemulsion polymerization in a solution of the cationic monomer [2-(methacryloyloxy)ethyl] trimethylammonium chloride under UV radiation at room temperature produced MSPBs. Finally, Pt-functionalized **MRC-12** was obtained upon addition of H₂PtCl₆ aqueous

solution followed by reduction with excess NaBH_4 . This catalyst exhibited high activity in the reduction of 4-NP in the presence of NaBH_4 in water, as shown by results of photometric monitoring. Analysis of kinetic data showed that the reaction was pseudo-first-order with respect to 4-NP. Additionally, the catalyst could be reused eight times without obvious decrease of the catalytic activity.

As an alternative, Li and coworkers¹⁸⁴ used polymer single crystals (PSCs) as magnetically recoverable support, and reported the use of PSC-supported Pt-functionalized **MRC-13** for the reduction of 4-NP in the presence of NaBH_4 in water. **MRC-13** was composed of PSCs, platinum nanoparticles, and Fe_3O_4 nanoparticles, acting as support, catalyst, and magnetic responsive material, respectively (Fig. 13). In this catalyst system, platinum nanoparticles and Fe_3O_4 nanoparticles were bonded to thiol groups and to hydroxyl groups on a tailor-designed polymeric single-crystal surface. Because of their quasi-two-dimensional nature, PSCs possessed high surface-area-to-volume ratio ($2.5 \times 10^8 \text{ m}^{-1}$), which efficiently enabled the high loading of platinum and Fe_3O_4 nanoparticles. This catalyst system ensured efficient reaction and reliable nanoparticle recycling for four runs. Furthermore, enhanced catalytic activity in the reduction of 4-NP in the presence of NaBH_4 in water were observed. This enhancement was ascribed to the synergistic interactions between platinum and Fe_3O_4 nanoparticles.

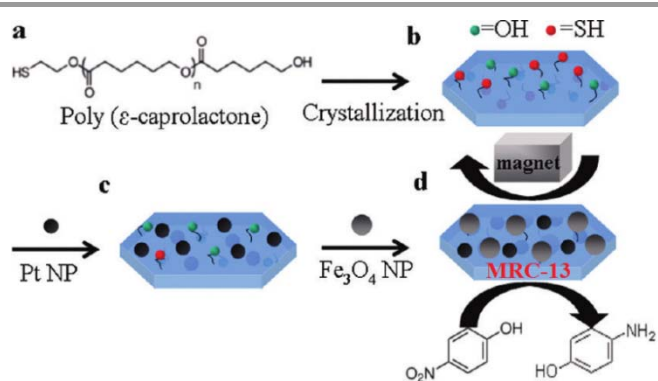


Fig.13 The schematic preparation of **MRC-13**.

3.1.8 Ru/Rh/Ir-functionalized MRCs: Ruthenium, rhodium, and iridium are widely used transition metals for catalyzed organic transformations. They are common catalysts for reactions such as hydrogenation, oxidation, isomerization, hydrolysis, as well as carbon–carbon bond formation. Only a few Ru/Rh/Ir-functionalized MRCs have been developed recently, for hydrolysis, hydrogenation, and asymmetric-transfer hydrogenation.

In an earlier work by Varma and coworkers,¹⁸⁵ a Ru-functionalized MRC was developed. In their work, they reported a convenient and inexpensive synthesis of ruthenium hydroxide catalyst supported on Fe_3O_4 nanospheres. They used dopamine as a robust anchor in the coordination of amine-functionalized Fe_3O_4 MNPs with ruthenium chloride under ultrasonication to form ruthenium hydroxide-functionalized

MRC. The benefits of the process are that Ru-functionalized MRC could be readily prepared from inexpensive starting materials in water with excellent yield. Furthermore, the sonochemical method could form highly dispersed ruthenium hydroxide species onto Fe_3O_4 MNPs. The Ru-functionalized MRC enabled to catalyze the hydration of nitriles with high yield and excellent selectivity in water. In addition, the Ru-functionalized MRC could be recovered and reused. Very recently, Varma and coworkers also used a SiO_2 -coating strategy to prepare a similar Ru-functionalized MRC,¹⁸⁶ which could be readily prepared in gram-level quantities in one step under ambient conditions in aqueous medium. Similarly, excellent catalytic activity in hydration of nitriles could also be obtained. Polshettiwar and coworkers¹⁸⁷ developed another MNP-based ruthenium(II)-arene derivative with 1,3,5-triaza-7-phosphatricyclo[3.3.1^{3,7}]decane as a ligand. The catalyst showed good catalytic activity and reusability for nitriles hydration, isomerization of allylic alcohols, and cycloisomerization of (*Z*)-enynols.

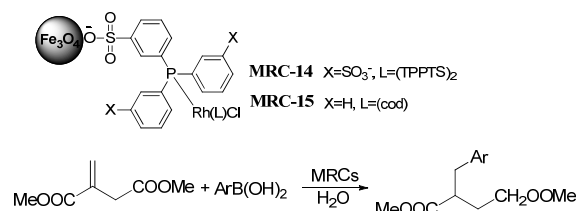


Fig. 14 The structures of MRCs and the catalytic addition reactions.

In contrast to Ru-functionalized MRC reported by Varma group¹⁸⁵, Rh-functionalized **MRC-14** and **MRC-15** (Fig. 14), were explored by Laska group.¹⁸⁸ In their work, a rhodium complex containing sulfonated ligands was directly anchored to the surface of Fe_3O_4 nanoparticles. Both **MRC-14** and **MRC-15** could promote the hydrogenation of olefins and the addition of arylboronic acids to dimethyl itaconate in water. **MRC-14** could be readily separated by use of a magnetic field and then used for >10 cycles of olefins in hydrogenation without loss of activity.

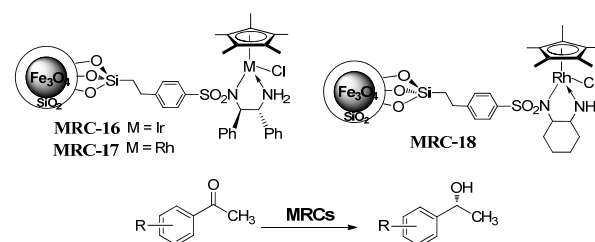


Fig. 15 The structures of MRCs and the catalytic asymmetric transfer hydrogenation.

Interestingly, Ru/Rh/Ir-functionalized MRCs could also be applied to asymmetric catalysis. Liu group^{189, 190} reported a convenient method for preparing three magnetic catalysts, **MRC-16**, **MRC-17**, and **MRC-18** (Fig. 15), through direct complexation of $[\text{Cp}^*\text{IrCl}_2]_2$ or $[\text{Cp}^*\text{RhCl}_2]_2$ with (*S,S*)-TsDPEN-modified (TsDPEN = *N*-(*p*-toluenesulfonyl)-1,2-

diphenylethylenediamine) SiO₂-coated Fe₃O₄ nanoparticles and [Cp*RhCl₂]₂ with (*R,R*)-TsDACH-modified (DACH = diaminocyclohexane) SiO₂-coated Fe₃O₄ nanoparticles. All synthesized catalysts exhibited excellent catalytic activity and enantioselectivity in the asymmetric transfer hydrogenation of aromatic ketones in water. These properties are comparable to those of their homogeneous counterparts. **MRC-16**, **MRC-17**, and **MRC-18** could be quantitatively recovered by using a small magnet and then reused for 10 runs without obviously affecting their enantioselectivity. Very recently, Liu group¹⁹¹ utilized a similar strategy to prepare a hydrophobic, Rh-functionalized MRC using the same complexation of [Cp*RhCl₂]₂ with (*S,S*)-TsDPEN-modified Fe₃O₄ nanoparticles. It only differed from the former method is that hydrophobic phenylene-coated Fe₃O₄ nanoparticles replaced SiO₂-coated Fe₃O₄ nanoparticles. The significant contribution of this phenylene-coated Rh-functionalized MRC is that this MRC could significantly boost asymmetric transfer hydrogenation because of its high hydrophobicity. Similarly, it also showed high enantioselectivity and good recyclability in the asymmetric transfer hydrogenation of aromatic ketones in water. As another alternative immobilization strategy, Li and coworkers¹⁹² reported Ru-functionalized MRC (using the same Ru-TsDPEN active species) prepared through a magnetic siliceous mesocellular foam approach. Similarly, this Ru-functionalized MRC also exhibited highly catalytic activities and good enantioselectivities in the asymmetric transfer hydrogenation of aromatic ketones. Furthermore, it could be reused for at least nine runs with reasonable loss of catalytic activity.

3.1.9 Sb-functionalized MRCs: Trivalent antimony ion, an inexpensive commercial reagent that is easy to handle, has recently attracted much attention for its ability to catalyze organic transformations such as Knoevenagel condensation, Michael addition, and ring opening of epoxides. Here, only a Sb-functionalized **MRC-19** reported by Zhang group¹⁹³ was applied in catalytic synthesis of *N*-substituted pyrroles. As shown in Fig.16, the reaction of aniline and tetrahydro-2,5-dimethoxyfuran in water catalyzed by **MRC-19** afforded the corresponding products in 95% yield without any side products. This Sb-functionalized MRC is also suitable for the catalytic Clauson–Kaas reaction and showed a high recyclability.

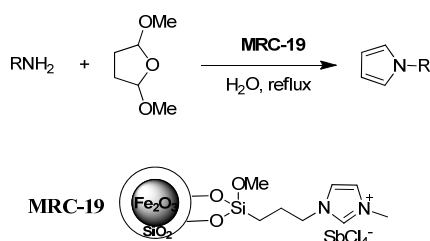


Fig.16 The syntheses of *N*-substituted pyrroles catalyzed by **MRC-19**.

3.1.10 W-functionalized MRCs: Heteropolyacids have been commercially utilized, mainly applying in petrochemical processes. Although lots of heteropolyacids employed in

catalysis could be recovered and reused, the immobilization of heteropolyacids onto magnetic materials only involves 12-Tungstophosphoric acids (H₃PW₁₂O₄₀). Recently, Rafiee and coworkers¹⁹⁴ reported a heteropolyacid-based W-functionalized MRC by immobilization of H₃PW₁₂O₄₀ on the surface of silica-encapsulated γ -Fe₂O₃ nanoparticles. This MRC are mostly spherical in shape and have an average size of approximately 94 nm. Interestingly, the MRC had an surface active sites that are more numerous than those of its homogeneous analogs. This feature confers high catalytic efficiency of the MRC in one-pot three-component Mannich-type reactions of aldehydes, amines, and ketones in water, resulting in up to 98% yield. Furthermore, the catalyst could be recovered and reused after at least five cycles without any significant loss of its catalytic activity. This kind of heteropolyacid-based MRC could also be used to construct 1,8-dioxo-9,10-diaryldecahydroacridines, 1,8-dioxooctahydroxanthenes, and 14-aryl-14*H*-dibenzo[*a,j*]xanthenes through above one-pot reaction in their recent study.¹⁹⁵

3.1.11 Organocatalyst-functionalized MRCs: Organocatalysts functionalized on magnetic supports have a broad range of applications in various organic transformations. Recent reviews have highlighted great achievements in this area. Significant advantages of magnetic organocatalysts are their easy recovery and reuse, which result in an environmentally benign catalytic process. Main strategies in constructing organic molecule-functionalized MRCs focus on traditional approaches, in which organic catalysts or ligands are grafted onto the surface of MNPs or SiO₂-coated MNPs.

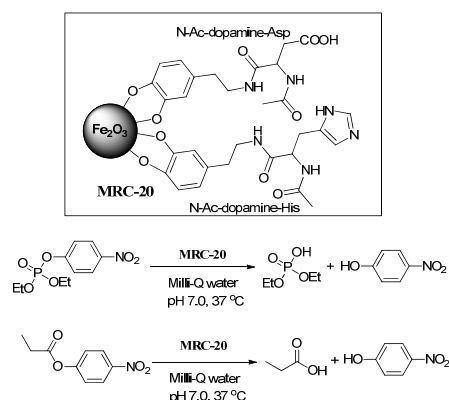


Fig.17 The structure of **MRC-20** and the hydrolysis of phosphoester and carboxylic ester.

Earlier work in immobilization of organic molecule onto Fe₂O₃ MNPs was developed by Gao group¹⁹⁶ at 2006. As shown in Fig. 17, they utilized dopamine as a linker for supporting two amino acid residues (Asp and His residues, which have a carboxylate group and an imidazole group on side chains, respectively). They also immobilized a mixture of two amino acid derivatives of dopamine (1:1 molar ratio of *N*-Ac-dopamine-Asp and *N*-Ac-dopamine-His) onto Fe₂O₃ MNPs (average size of 12 nm), forming the Asp-His-functionalized **MRC-20**. **MRC-20** is a magnetic biomimetic nanocatalyst that

exhibited high activity in the hydrolysis of paraoxon (phosphoester) and 4-nitrophenyl acetate (carboxylic ester) in milli-Q water (pH 7.0) at 37 °C. The hydrolyzed amount of paraoxon could be converted to 77% after 48 h and increased to 92% after 96 h, which is markedly higher than the amount obtained by using the corresponding pair without a nanoparticle support. The enhanced activity is attributed to the carboxylate–imidazole cooperativity induced by the close proximity of the carboxylate–imidazole pair on the surface of the nanoparticle. Moreover, **MRC-20** could be recovered easily and reused for at least four times without apparent decrease in conversion.

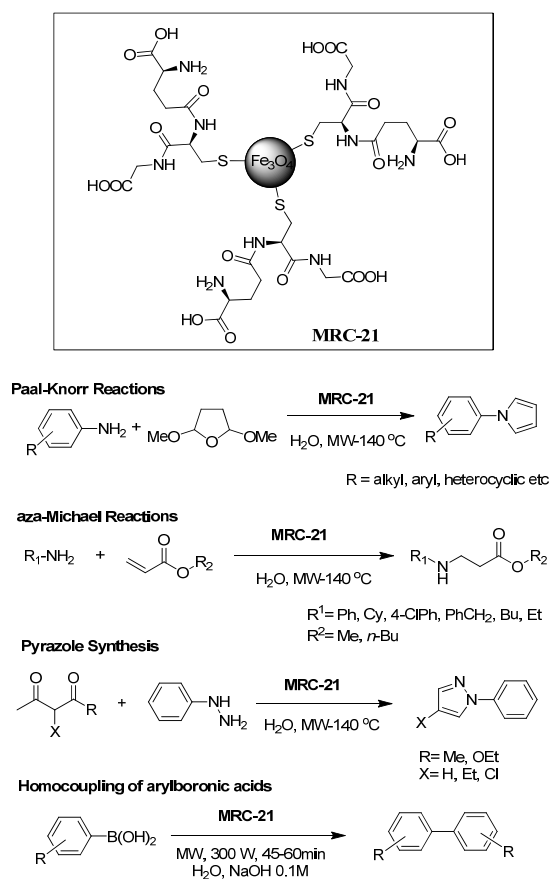


Fig.18 The structure of **MRC-21** and the catalytic reactions.

Developments in organic molecule-functionalized MRCs were furthered by Polshettiwar and Varma group.^{197,198} Through a sonochemical strategy, they used glutathione as organocatalyst and anchored it onto the surface of Fe₃O₄ MNPs *via* coupling of its thiol group with the free hydroxyl groups of Fe₃O₄ surfaces. The resulting magnetic glutathione-functionalized organocatalyst (**MRC-21**) showed highly efficiency in the Paal–Knorr synthesis of pyrrole heterocycles in water under microwave radiation (Fig.18). Reusability test for **MRC-21** indicated that it could be separated easily and reused at least five times without any change in activity. It also showed high catalytic performance in aza-Michael reactions and in synthesis of pyrazole. Also, Leque and coworkers²⁴ extended the use of **MRC-21** to catalyze homocoupling of various

arylboronic acids. In this reaction, electron-donating or -withdrawing substituents at the ortho or para position of aryl groups could be smoothly converted to products with good yields. In addition, the recycled catalyst could be used in a repeat reaction without any appreciable loss of activity.

Also, Nemati group¹⁹⁹ reported SiO₂-coated sulfonic acid-functionalized MRC (Fe₃O₄@SiO₂-SO₃H) (Fig.19). This catalyst was used in the synthesis of various tetraketone derivatives *via* Knoevenagel condensation and Michael addition in water. Extended-scope experiments showed that the reaction of a variety of arylaldehydes with dimedone, or 1,3-indanedione, or 1,3-dimethylbarbituric acid resulted in the formation of the corresponding products in high yields. Interestingly, reactions of benzaldehydes bearing strongly electron-donating groups and 1,3-indanedione or 1,3-dimethylbarbituric acid only produced the Knoevenagel condensation products. Furthermore, Fe₃O₄@SiO₂-SO₃H could be readily recovered by using a simple external magnet and reused three times without any significant loss of activity. Very recently, they²⁰⁰ extended the use of Fe₃O₄@SiO₂-SO₃H to the one-pot three-component catalytic synthesis of pyrimido[4,5-*b*]quinolines and indeno-fused pyrido[2,3-*d*]pyrimidines in water under mild conditions (Fig. 20). Results indicate that Fe₃O₄@SiO₂-SO₃H possessed good catalytic performance, producing yields of 81% to 95%. It could be recovered completely and its catalytic efficiency remained unaltered after three cycles, giving the one-pot method potential use in large-scale synthesis.

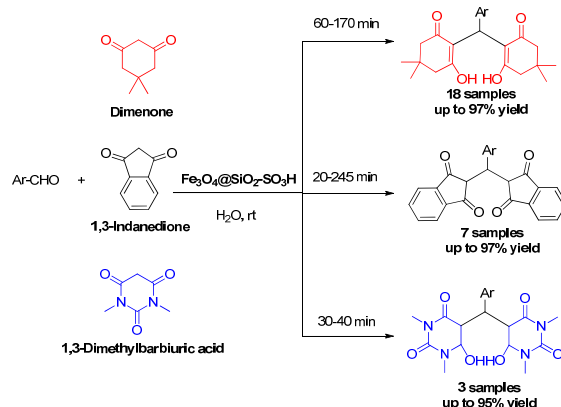


Fig.19 The syntheses of tetraketones catalyzed by Fe₃O₄@SiO₂-SO₃H.

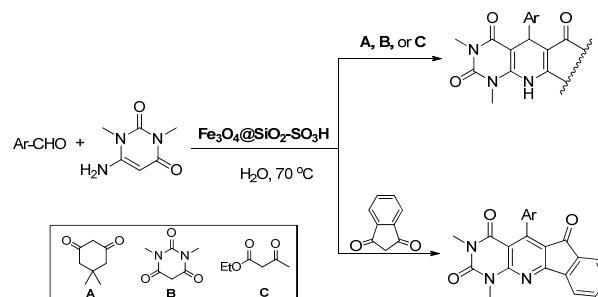


Fig.20 The syntheses of pyrimido[4,5-*b*]quinolines and pyrido[2,3-*d*]pyrimidines catalyzed by Fe₃O₄@SiO₂-SO₃H.

Interestingly, SiO₂-coated dodecyl benzenesulfonic acid-functionalized MRC was also applied to the one-pot, three-component catalytic reactions reported by Liu and Zhang group.²⁰¹ In their work, γ -Fe₂O₃ was coated with SiO₂ and then dodecyl benzenesulfonic acid (DDBSA) was grafted on the particle surface to form the magnetic catalyst, γ -Fe₂O₃@SiO₂-DDBSA. Catalytic reactions of barbituric acids, isatins and cyclohexane-1,3-diones in water were investigated (Fig.21). Results of this study indicate that the catalyst possessed high performance in conversion of the various substrates to a library of spirooxindole–pyrimidine derivatives. Furthermore, this water reaction medium, easy recovery of the catalyst using an external magnet, and high yields with up to six recycles make the protocol sustainable and economic.

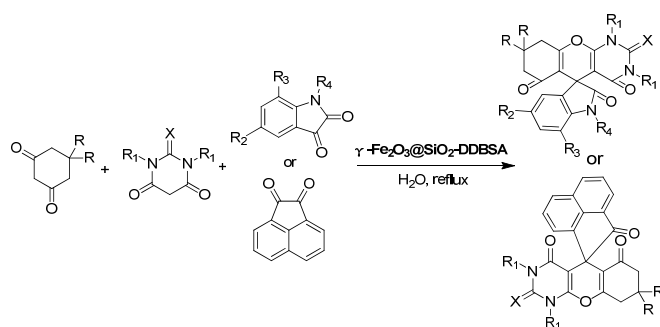


Fig.21 The syntheses of 8,9-dihydrospiro[chromeno[2,3-*d*]pyrimidine-5,3'-indoline] and spiro[acenaphthylene-1,5'-chromeno[2,3-*d*]pyrimidine] derivatives catalyzed by γ -Fe₂O₃@SiO₂-DDBSA.

Very recently, two other sulfonic acid-functionalized MRCs were also studied. Qi group²⁰² synthesized such MRCs by incomplete hydrothermal carbonization of cellulose followed by Fe₃O₄ grafting and –SO₃H group functionalization. The resulting catalyst contained –SO₃H, –COOH, and phenolic –OH groups. This material exhibited good catalytic activity in the hydrolysis of cellulose in either an ionic liquid phase or water-only phase. A total reducing sugar yield of 51% was obtained by reaction in water at 180 °C for 9 h. The catalyst was easily separated from the reaction products by using an external magnetic field. Meanwhile, He group²⁰³ prepared a carbon-coated sulfonic acid-functionalized MRC with core-shell structure (Fe₃O₄@C-SO₃H) and applied it to the hydrolysis of cellulose. Their results show that this catalyst had high activity, leading to 48.6 % cellulose conversion after 12 h and 52.1% glucose selectivity in the reaction performed at 140 °C. It could be reused three times with only a slightly decrease in activity.

Using alternative methods, Rostami group²⁰⁴ directly immobilized *N*-propylsulfamic acid onto Fe₃O₄ nanoparticles to construct a propylsulfamic acid-functionalized **MRC-22**. **MRC-22** was obtained through reaction of aminopropyl-functionalized MNPs and chlorosulfuric acid in CH₂Cl₂ at room temperature. It was used in the catalytic synthesis of 2-substituted 2,3-dihydroquinazolin-4(1*H*)-ones by direct cyclocondensation of anthranilamide with aldehydes and ketones in water (Fig. 22). The results show that **MRC-22**

exhibited excellent catalytic activity, resulting in yields of up to 97%. Moreover, **MRC-22** could be reused for up to 10 cycles without significant loss of activity.

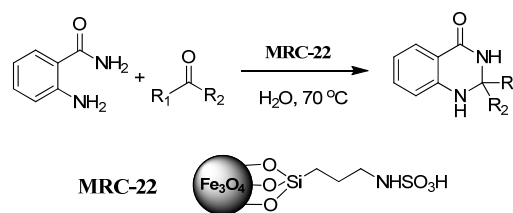


Fig. 22 The structure of **MRC-22** and the catalytic syntheses of 2,3-dihydroquinazolin-4(1*H*)-ones.

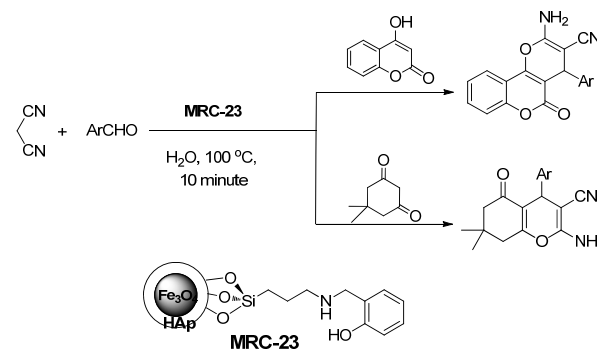


Fig.23 The structure of **MRC-23** and the catalytic syntheses of 4*H*-benzo[*b*]pyrans and dihydropyrano[*c*]chromenes.

Apart from the aforementioned sulfonic acid-functionalized MRCs, other organocatalyst-functionalized MRCs were also studied. Shafiee and coworkers²⁰⁵ reported (2-aminomethyl)phenol-functionalized **MRC-23**, and its application in the synthesis of 4*H*-benzo[*b*]pyrans and dihydropyrano[*c*]chromenes. This catalyst could be easily prepared by grafting of 2-hydroxybenzaldehyde onto the surface of amino-functionalized, hydroxyapatite-coated MNPs followed by reduction with excess NaBH₃CN in dry MeOH. As shown in Fig. 23, this catalyst exhibited high catalytic activity in the one-pot, three-component catalytic synthesis of dihydropyrano[*c*]chromene and 4*H*-drobenzo[*b*]pyran in water. The advantage of this catalyst is that it could be recovered simply with an external magnet and reused in 10 successive runs with no significant structural change and loss of activity.

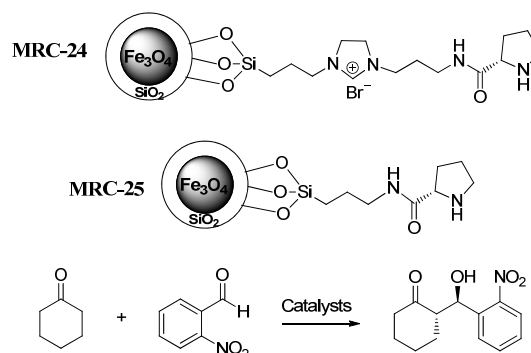


Fig. 24 The structures of MRCs and the asymmetric adol reaction.

Proline is widely used in catalysis reactions, especially in asymmetric aldol reactions. Tan and coworkers²⁰⁶ prepared two chiral proline-functionalized **MRC-24** and **MRC-25** (Fig. 24), which was used in the asymmetric aldol reaction in water. In contrast to **MRC-25**, **MRC-24** could be dispersed more uniformly in water to form a stable suspension. This ability is ascribed the nanoscale size of the supports and the high solubility of imidazolium ion. These features impart markedly higher catalytic activity to **MRC-24** compared with that of **MRC-25** and L-proline in asymmetric aldol reaction in water. Moreover, **MRC-24** showed high catalytic activity in the aldol reaction of a wide range of ketones and aromatic aldehydes in water.

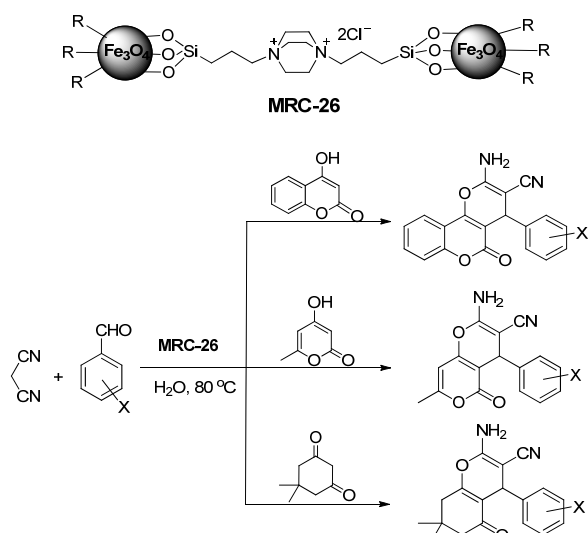


Fig. 25 The structure of **MRC-26** and the catalytic synthesis of 4H-benzo[b]pyran derivatives.

Very recently, Kiasat group²⁰⁷ immobilized double-charged diazoniabicyclo[2.2.2]octane dichloride (DABCO) onto Fe_3O_4 nanospheres to prepare a DABCO-functionalized **MRC-26**. **MRC-26** was prepared by ammonia-catalyzed hydrolysis of alkoxy silane groups of double-charged DABCO and tetraethylorthosilicate on Fe_3O_4 spheres. The catalytic activity was probed through one-pot synthesis of pyran annulated heterocyclic compounds *via* three-component coupling of aromatic aldehydes, malononitrile, and β -diketones (4-hydroxycoumarin, dimedone, and 4-hydroxy-6-methyl-2-pyrone) in water (Fig. 25). The results show that the multicomponent reactions proceeded when aromatic aldehydes with both electron-withdrawing and electron-donating functionalities were used. Furthermore, reactions using enol tautomers (4-hydroxycoumarin and 4-hydroxy-6-methyl-2-pyrone) proceeded smoothly, giving high yields. **MRC-26** could also be readily separated from the reaction system by using an external magnet and then directly reused.

Interestingly, a TEMPO-functionalized **MRC-27** (TEMPO: 1-hydroxy-4-oxo-2,2,6,6-tetramethylpiperidine), was reported by Karimi group.²⁰⁸ In their work, **MRC-27**, which had a core-shell structure, was prepared through reductive amination of

amino-functionalized SiO_2 -coated magnetic nanoparticles and TEMPO in the presence of NaBH_3CN . As shown in Fig. 26, this magnetic catalyst showed high activity in the aerial oxidation of acid-sensitive, sterically hindered alcohols. A significant advantage of this synthesis was that the products without any chromatographic purification could reach >99%, which is not generally unachievable with most halogen-based TEMPO-catalyzed protocols. Furthermore, this catalytic system couples the advantages of heterogeneous systems, which enable easy separation and good reusability (up to 20 runs), and of homogeneous TEMPO-based systems, which impart high activity and reproducibility. These advantages give the system potential use in large-scale applications.

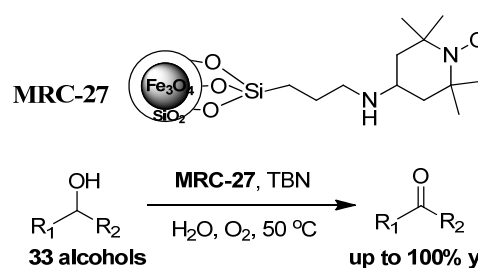


Fig. 26 The structure of **MRC-27** and the catalytic oxidation of alcohols.

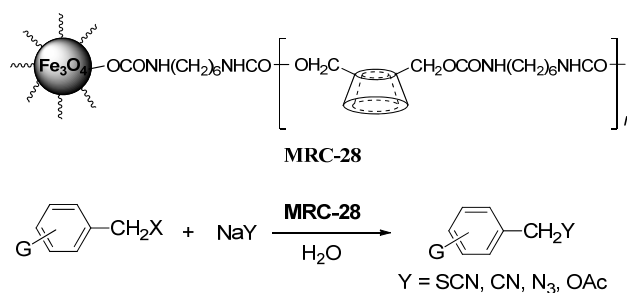
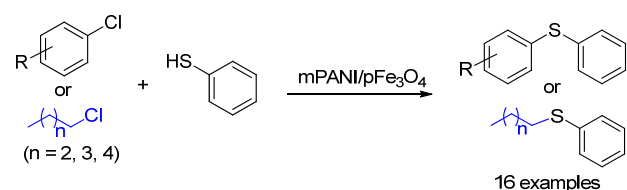


Fig. 27 The structure of **MRC-28** and the catalytic nucleophilic substitution.

Another interesting example of MRC is cyclodextrin-polyurethane-functionalized **MRC-28** developed by Kiasat group.²⁰⁹ In their work, grafting of β -cyclodextrin onto the surface of the polyurethane-coated MNPs using isocyanate groups afforded then cyclodextrin-polyurethane-functionalized catalyst **MRC-28** (Fig. 27). The authors used the reaction of benzyl halides with thiocyanate anion in water to investigate the catalytic performance of **MRC-28** in nucleophilic substitution. Their results demonstrate that **MRC-28** could increase the rate of the nucleophilic substitution in water. A scope experiment using various substrates was subsequently conducted, and clean reactions were observed in all cases. Moreover, **MRC-28** could be reused for at least 10 times without significant loss of activity. Very recently, they reported another similar cyclodextrin-polyurethane-functionalized MRC²¹⁰ that exhibited high activity in the synthesis of benzyl thiocyanates and azides. Meanwhile, Lu and coworkers²¹¹ also immobilized β -cyclodextrin on SiO_2 -coated Fe_3O_4 nanoparticles and applied the nanoparticles to the synthesis of aldehydes through reaction of primary benzylic

alcohols and several heterocyclic alcohols using NaOCl as oxidant.

S-arylation of chlorides with thiophenol



C-S bond formation between thiourea and aryl halides

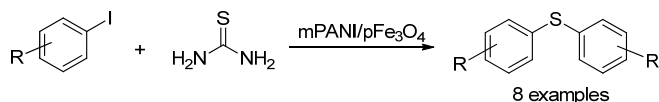


Fig.28 The mPANI/pFe₃O₄ catalyzes S-arylations and C-S bond formation reactions.

In addition, Likhar group²¹² reported a polyaniline-functionalized MRC (mPANI/pFe₃O₄, mPANI = mesoporous polyaniline) and its application in catalytic C-S bond formation, as shown in Fig. 28. In their work, they functionalized Fe₃O₄ nanoparticles with 3-aminopropyltrimethoxysilane. The mPANI-coated Fe₃O₄ microspheres were then obtained by *in situ* surface polymerization in the presence of PVP and sodium dodecyl benzene sulfonate. The mPANI/pFe₃O₄ microspheres were able to synthesize various unsymmetrical diaryl sulfides in S-arylation of aryl, alkyl and heterocyclic halides with thiophenol in water. Also, the microspheres enabled selective synthesis of symmetrical diaryl sulfides through S-arylation of various aryl iodides with thiourea in water. Moreover, they could be easily recovered by use of an external magnetic field and reused repeatedly for at least five cycles without obvious decrease in catalytic activity.

Table 5 Classifications of catalytic species in a cosolvent phase of water-and-organic solvent.

Types of Catalyst	Catalyst	Organic transformation	Reference
Metal/Organometal catalyst			
Mn		Oxidation	213, 214
Pd		Coupling reaction Reduction Hydrogenation	215–224
Organocatalyst			
		Asymmetric dihydroxylation	225
	ammonium and phosphonium salts	Coupling halogen exchange	226
		Condensing reaction	227
		Reduction	228

ARTICLE

3.2 Organic transformation in a cosolvent phase of water-and-organic solvent

Generally, cosolvent phase of water-and-organic solvent increases the solubility of organic reactants in water and enhances catalytic efficiency for organic transformations catalyzed by MRCs. Cosolvent phases mainly involve EtOH–H₂O, acetone–H₂O, DMF–H₂O, CH₃CN–H₂O and so on. In this section, we summarize MRCs in cosolvent reaction systems, covering Mn-catalyzed oxidation, Pd-catalyzed coupling or reduction or hydrogenation, and a few organic molecule-catalyzed asymmetric dihydroxylation, condensing and reduction reactions (table 5).

3.2.1 Mn-functionalized MRCs: As mentioned above, manganese complexes are widely used as catalysts for oxidation. Two Mn-functionalized MRCs were developed and applied to catalytic oxidation in a CH₃CN–H₂O cosolvent. Tangestaninejad and co-workers²¹³ reported a SiO₂-coated porphyrinatomanganese(III) functionalized **MRC-29** (Fig. 29), which was highly efficient in the epoxidation of alkenes and hydroxylation of alkanes and could be reused for at least six times without significant loss of its activity.

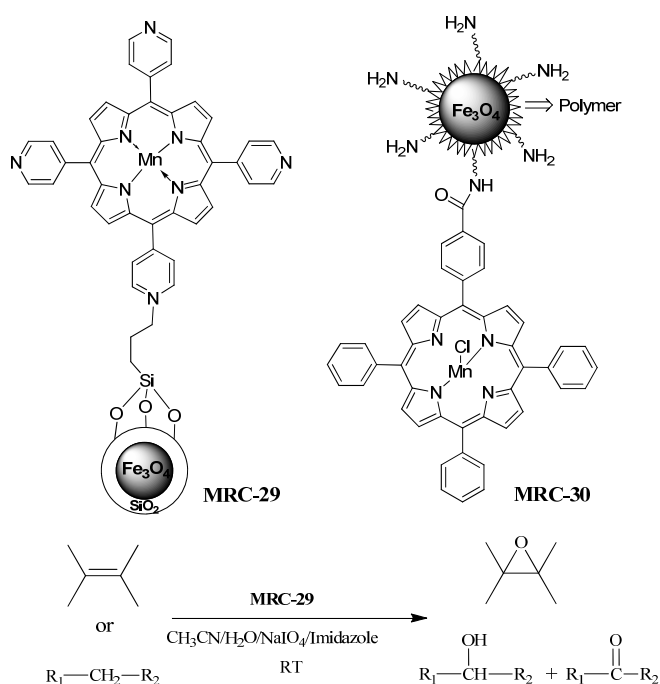


Fig. 29 The structures of MRCs and the catalytic epoxidation of alkenes and hydroxylation of alkanes.

Another Mn-functionalized MRC was reported Jiang group.²¹⁴ It was mainly applied to the epoxidation of cyclooctene and cyclohexene as a probe reaction in a CH₃CN–H₂O cosolvent. The only difference of this method from the aforementioned epoxidation is that they used MNPs coated with poly(glycidyl methacrylate). This Mn-functionalized **MRC-30** was obtained through amide bond to link manganese(III) 5-(4-carboxyphenyl)-10,15,20-triphenylporphyrin chloride (Fig. 29).

3.2.2 Pd-functionalized MRCs: Pd-functionalized MRCs are well-known catalysts for C–C bond formation in water-only phase. In this section, we focus on traditional coupling reaction and hydrogenations catalyzed by Pd-functionalized MRCs invarious cosolvent systems.

Earlier work on applications of Pd-catalyzed Heck-coupling reactions in a CH₃CN–H₂O system was reported by Hegroup.²¹⁵ They utilized traditional three-step synthesis to prepare SiO₂-coated Pd-functionalized MRC. In this process, Fe₃O₄ nanoparticles were embedded in silica through the Stöber method. The SiO₂-coated MNPs were then modified with 3-aminopropyltriethoxysilane. Finally, Pd-functionalized MRC was obtained by bonding the synthesized Pd colloid with the pendant amine group onto SiO₂-coated MNPs. This Pd-functionalized MRC had better catalytic efficiency in the cross coupling of acrylic acid with iodobenzene in a CH₃CN–H₂O cosolvent (1:3, v/v) compared with that of carbon-supported palladium catalysts. The high catalytic performance is attributed to the uniform distribution of palladium nanoparticles on the surface of the SiO₂-coated MNPs. Also, Song group²¹⁶ prepared SiO₂-coated Pd-functionalized MRC through immobilization of palladium nanoparticles onto the surface of amine-functionalized MNPs modified with ionic liquid. This MRC exhibited high catalytic activity in Suzuki coupling reactions of a wide range of aryl halides and arylboronic acids in an EtOH–H₂O cosolvent. The catalyst could be easily recovered magnetically from the reaction mixture and could be reused for several times without significant loss of activity.

An improved SiO₂-coated Pd-functionalized **MRC-31A** was also prepared by Li group²¹⁷ using the glycerol as stabilizer and applied in Suzuki and Heck reactions in a DMF–H₂O (1:2 v/v) cosolvent (Fig. 30). To avoid leaching of Pd, they prepared highly dispersible palladium nanoparticles through sequential attachment of glycerol and chlorodiphenylphosphine onto SiO₂-coated Fe₃O₄, followed by treatment with hydrazine hydrate in an ethanolic solution of palladium chloride. Compared with the aforementioned magnetic Pd-loaded catalyst, this Pd-functionalized SiO₂-coated magnetic catalyst showed enhanced catalytic activities in both Suzuki and Heck reactions in the

presence of low Pd loading (0.76 mol % for Suzuki coupling and 0.95 mol % for Heck coupling). Also, the catalyst had high recyclability; it could be reused for at least six times without noticeable loss of its activity. Notably, the protection by glycerol played an important role in preventing leaching of Pd, resulting in high recyclability.

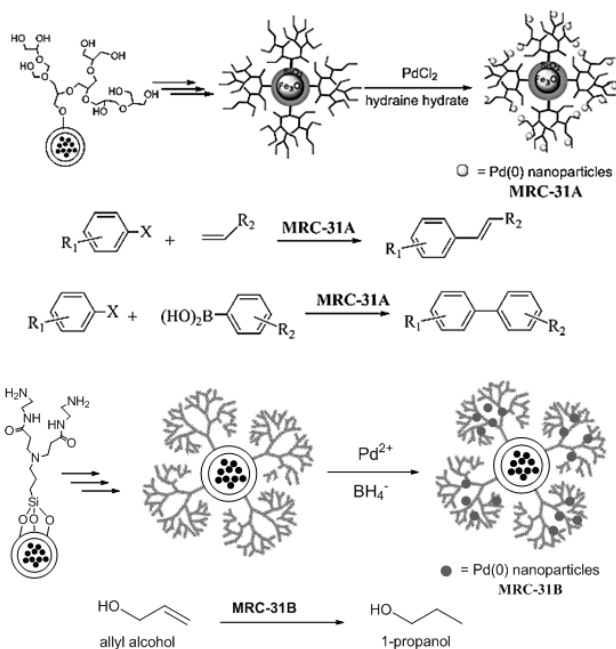


Fig. 30 The schematic preparation of MRCs, the catalytic Suzuki, Heck reactions and hydrogenations.

Similarly, Gao group²¹⁸ also reported a SiO₂-coated Pd-functionalized **MRC-31B** used in the application of Pd-catalyzed hydrogenation of allyl alcohol in a MeOH–H₂O cosolvent (4:1 v/v). As shown in Fig.30, the first-generation dendrimers were prepared through a procedure, in which methyl acrylate was combined with synthesized amine-functionalized magnetic particles through Michael addition followed by reaction with ethylenediamine. The second-, third-, and fourth-generation dendrimers were obtained by repeating those steps. **MRC-31B** was synthesized by supporting (NH₄)₂PdCl₄ on the as-prepared dendrimers and subsequently reducing them with NaBH₄. TEM images of **MRC-31B** based on the fourth-generation dendrimers show that the magnetic particles have sizes of about 60–100 nm and that nanosized Pd particles with uniform size (about 2.5 nm) are well dispersed. **MRC-31B** led to high conversions and selectivity toward hydrogenation of allyl alcohol to 1-propanol. These characteristics are ascribed to the highly dispersible palladium nanoparticles within PAMAM. **MRC-31B** could be reused for at least five times without noticeable loss of its activity. Notably, amine groups of branched polyethylenimine on the SiO₂-coated MNPs surface allowed entrapment of Pd nanoparticles and prevent metal leaching during the reaction, resulting in recyclability of the catalyst without any loss of activity.

Interestingly, Luo group²¹⁹ utilizes “click” method to prepared a SiO₂-coated Pd-functionalized **MRC-32** (Fig. 31) for application in Suzuki–Miyaura reactions in an EtOH–H₂O cosolvent. **MRC-32** was synthesized *via* copper-catalyzed ligation of an alkynylated-imino-pyridine ligand with azide-functionalized silica-coated Fe₃O₄ nanoparticles followed by treatment with a methanolic solution of Na₂Pd₂Cl₆. **MRC-32** exhibited high efficiency in the reactions of various aryl bromides with arylboronic acids, with K₂CO₃ as base in an EtOH–H₂O cosolvent (1:1, v/v) at 60 °C in air. The recyclability of **MRC-32** was investigated by using different volume ratios of EtOH/H₂O. The catalytic performance could be retained for a few more cycles when the less water was used as the reaction solvent. Very recently, Khosropour and co-workers²²⁰ also reported another Pd-functionalized MRC with the ligand of N-heterocyclic carbene. The catalyst exhibited high activity in Suzuki–Miyaura cross coupling reactions a DMF–H₂O cosolvent.

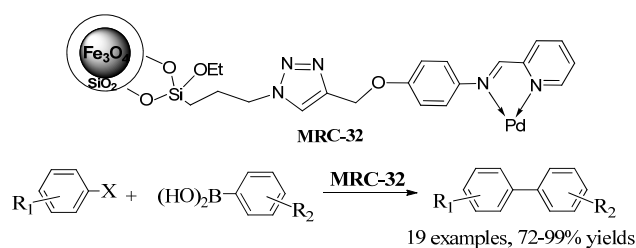


Fig. 31 The structure of MRC-32 and the catalytic Suzuki reactions.

Also, palladium nanoparticles could be immobilized onto Fe₃O₄ nanoparticles encapsulated with nickel silicate-shell. Xuan group²²¹ reported this Pd-functionalized MRC (MP@NiSiO/Pd) with a rattle nanostructure. Magnetic core particles rattle encapsulated with a nickel silicate shell (MP@NiSiO) were synthesized by using a facile templating method. Pd nanoparticles of various sizes could be directly immobilized onto the MP@NiSiO rattles without use of any surfactant or capping reagent. MP@NiSiO exhibited good catalytic activity and could be reused for five times in Suzuki coupling reaction in a DME–H₂O cosolvent.

It is worth mentioning that palladium nanoparticles could be immobilized onto the surface of amine-terminated Fe₃O₄ without encapsulation in a silica sphere. Varma group applied them in Heck-type arylation in a PEG(400)–H₂O cosolvent.²²² Their synthetic method is strongly similar to that reported in the literature.¹⁷³ The key step in this route is the anchoring of dopamine (Dopa) molecules on the surface of Fe₃O₄ using sonication. Dopamine on the surface of iron was a suitable anchor, preventing leaching of the metal and functioning as a pseudo-ligand. The obtained catalyst (Fe₃O₄–Dopa–Pd) exhibited high catalytic activity in Heck-type arylation of terminal alkenes with diaryliodonium salts in aqueous polyethylene glycol under ultrasonication. In addition, this catalytic reaction could be applied to various substrates to produce high yields of products, including unactivated alkenes such as styrene, allyl acetate, and allyl alcohol. Similar to the

catalyst prepared by He group²¹⁵, $\text{Fe}_3\text{O}_4\text{-Dopa-Pd}$ could only be used in three consecutive cycles of reactions because of its same properties.



Fig.32 The schematic preparation of **MRC-33**, the catalytic Suzuki reactions and the catalytic reductions.

As an alternative, palladium nanoparticles were also immobilized onto the magnetically hollow-shell structural nanocomposite reported by Hyeon group²²³ as shown in Fig.32. In their work, pyrrole, a carbon precursor, was coated on the Fe_3O_4 hollow-shell nanostructure through chemical polymerization using palladium(II) nitrate as an oxidant. This step was followed by calcination of the synthesized nanocomposites to form Pd-functionalized **MRC-33**. An important feature of this catalyst is that the carbon coating (~25 nm thickness) prevents the hollow magnetic nanocomposite stable from collapsing. The palladium nanoparticles are dispersed on the carbon layer. **MRC-33** exhibited excellent catalytic activity in nitroarenes reduction and in Suzuki cross-coupling reactions because of its high surface area, which accommodates large amounts of small palladium nanoparticles. In addition, the porous carbon layer is permeable to organic reagents and improves the diffusion of substrates and products, resulting in high catalytic efficiency. The benefit of this synthetic process is that it offers a practical approach to load various metals such as Pd, Pt, and Rh on nanocomposites used for various catalytic reactions.

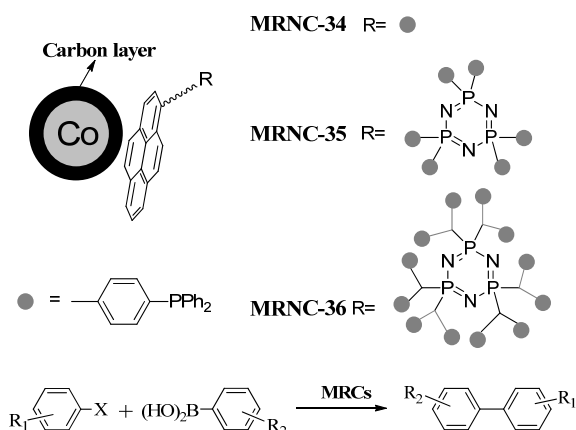
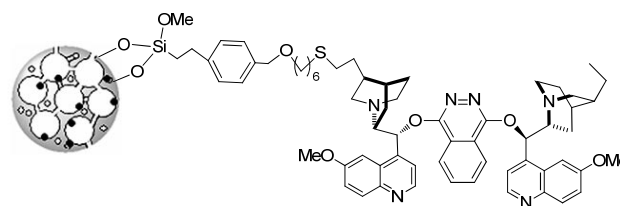


Fig. 33 The structures of **MRCs** and the catalytic Suzuki reactions.

Apart from magnetic Fe_3O_4 nanoparticles, magnetic cobalt nanoparticles could also function as supports in the construction of **MRCs**. A typical Pd-functionalized **MRC** was reported by Ouali and coworkers.²²⁴ They applied it to Suzuki reactions in a $\text{THF-H}_2\text{O}$ (2:5, v/v) cosolvent. In their work, they used carbon-coated cobalt nanoparticles as a support and grafted pyrene-tagged dendritic Pd-phosphine catalysts onto carbon-coated cobalt nanoparticles *via* $\pi\text{-}\pi$ stacking to construct novel Pd-functionalized **MRCs** (**MRC-34**, **MRC-35**, and **MRC-36**). As shown in Fig.33, these catalysts had triple functions; attachment of a dendritic ligand onto the MNP surface, which enables higher loading (0.5 mmol g^{-1} active sites); $\pi\text{-}\pi$ stacking of pyrene-functionality, which allows catalysis to proceed in the homogeneous phase; and use of a magnetic support, which enables facile agitation and recovery of the catalyst by use of an external magnetic field. These catalysts were assessed for activity and recyclability in Suzuki reactions. The results show that **MRC-35** could lead to good to excellent yields of products (70–98%). It could efficiently enhance Suzuki cross-coupling of PhBr and PhB(OH)₂ to 1,1'-biphenyl with an enhanced TON value. Also, it could be reused for up to 12 cycles without any significant loss of catalytic activity. This characteristic enables a practical recycling process in the preparation of Felbinac at 10 g level over multiple runs, meeting the specification limits for metal residues in the pharmaceutical industry.



MRC-37

Fig. 34 The structure of **MRC-37**.

3.2.3 Organocatalyst-functionalized **MRCs**:

Organocatalyst-functionalized **MRCs** applied to various catalytic reactions in water pose an environmental friendly process. In many cases, however, the insolubility of organic substrates in water reduces the efficiency of organic transformations. The use of a cosolvent of water-and-organic solvent may increase the solubility of organic reactants in water, thereby enhancing the catalytic efficiency. Earlier work on organocatalyst-functionalized **MRCs** was reported by Kim and co-workers.²²⁵ They utilized a magnetic carrier by impregnating $\text{Fe}(\text{NO}_3)_3$ into hierarchically mesocellular mesoporous silica to immobilize a cinchona alkaloid, forming a cinchona-functionalized **MRC-37** (Fig. 34). Asymmetric dihydroxylation of styrene and its derivatives in a *t*-BuOH- H_2O (1:1, v/v) cosolvent was investigated by employing OsO_4 and $\text{K}_3\text{Fe}(\text{CN})_6$ as oxidants. **MRC-37** presented almost the same reactivity and enantioselectivity as those of its homogeneous counterpart. The benefits for the cinchona-functionalized **MRC-37** in this case should be attributed to the well-connected three-dimensional pore structures and small particle size of the

mesostructured silica support, in which the site-isolated active sites on the surface and good accessibility to substrates are responsible for its highly catalytic efficiency. Furthermore, the high enantioselectivity could be maintained after eight cycles of use.

Meanwhile, Sato and coworkers²²⁶ also reported a series of quaternary ammonium- and orphosphonium-functionalized MRCs. These MRCs were prepared by directly grafting quaternary ammonium- or phosphonium-derived silane onto magnetic Fe₃O₄ nanoparticles. The feature of these MRCs could function as phase-transfer catalyst because of their quaternary ammonium or phosphonium salts, which could greatly promote catalytic transformations in aqueous medium. Catalytic coupling of PhONa with *n*-BuBr in a biphase of toluene-H₂O cosolvent could afford the corresponding products with good yields, which were comparable to those obtained with tetra-*n*-butylammonium iodide. In addition, halogen exchange of 1-bromooctane could be performed at high activity in the toluene-H₂O cosolvent. In contrast to the general phase-transfer catalysts, the significant advantage of these quaternary ammonium or phosphonium-functionalized MRCs is easy and rapid separation using an external magnet and repeated use, which are impossible with non-magnetic phase-transfer catalysts.

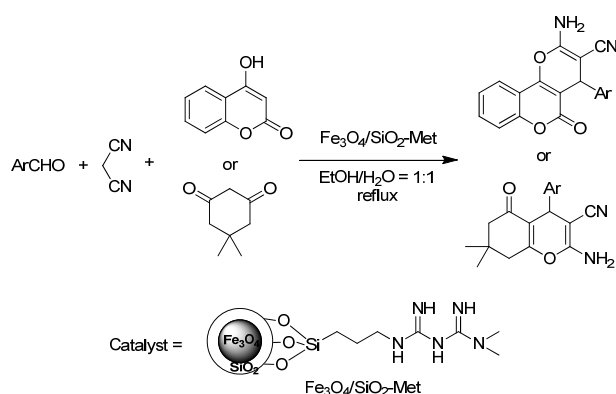


Fig.35 The syntheses pyran derivatives catalyzed by Fe₃O₄/SiO₂-Met.

Recently, Alizadeh and coworkers developed a SiO₂-coated biguanide-functionalized MRC(Fe₃O₄/SiO₂-Met)²²⁷ used for one-pot synthesis of pyran derivatives in aqueous ethanol. As shown in Fig.35, the catalytic performance of Fe₃O₄/SiO₂-Met was evaluated by preparation of 2-amino-4-aryl 3-cyano-5-oxo-4*H*,5*H*-pyrano[3,2-*c*]chromene derivatives. Synthesis was done by condensing 4-hydroxycoumarin, aldehydes, and malononitriles in EtOH-H₂O mixture (1:1, v/v) under reflux. More than 84% isolated yields were obtained. Furthermore, three-component reactions of dione, aldehydes, and malononitrile in the preparation of tetrahydrobenzo[*b*]pyrans also proceeded smoothly, producing 92% yield. In addition, Fe₃O₄/SiO₂-Met could also be applied to the nitroaldol reactions. Sequential reactions under mild conditions demonstrated the high stability, activity, and reusability of Fe₃O₄/SiO₂-Met. Moreover, the MRC could be recovered with

an external magnet and reused at least six times without obvious loss of activity in a three-component model reaction of 4-nitrobenzaldehyde, malononitrile, and 4-hydroxycoumarin.

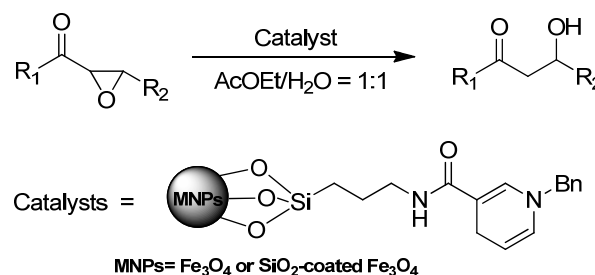


Fig.36 The structures of MRCs and the catalytic reductions.

Very recently, Xu and coworkers²²⁸ also reported two BNAH-functionalized MRCs (BNAH: 1-benzyl-1,4-dihydronicotinamide). As shown in Fig. 36, both BNAH-functionalized MRCs showed efficient activity in catalytic reduction of α,β -epoxy ketones in a biphase of AcOEt-H₂O (1:1, v/v) cosolvent. SiO₂-coated BNAH-functionalized MRC exhibited slightly higher activity in the reduction of phenyl(3-phenyloxiran-2-yl)methanone compared with that of bare BNAH-functionalized MRC. This difference might be due to the slight aggregation of bare BNAH-functionalized MRC. Furthermore, the SiO₂-coated BNAH-functionalized MRC could reduce various substrates (up to 16 other α,β -epoxy ketones), providing the corresponding reduction products with good to excellent yield. The SiO₂-coated BNAH-functionalized MRC could be separated simply and reused at least six times with little change in the catalytic efficiency in the reduction of 4-bromophenyl-3-phenyloxiran-2-yl-methanone.

4. Summary and outlook

During the past few decades, investigations of a wide variety of MNPs-based nanostructured catalysts and their applications in various organic transformations in aqueous medium have obtained great achievements. Numerous excellent magnetic heterogeneous catalysts have been developed and some have mimicked the structural properties of real catalytic surfaces, providing fundamental insight into heterogeneous catalysis. In most cases, these magnetic catalysts have exhibited catalytic activity comparable to or better than those of the corresponding homogeneous catalysts. Applications in various kinds of organic reactions have involved C-C coupling, hydrogenation, reduction, oxidation, acid-base catalysis, asymmetric catalysis, and biocatalytic reactions and so on, which can be recovered with an external magnet and reused repeatedly.

However, there are still a number of challenges in the use of MRCs in future research. These mainly focus on the following: (1) Molecular-level knowledge based on the structure-activity relationship is critical in the rational design of new MRCs. Although some effects of the support such as confinement effect, quantum size effect, and cooperative effects have been explored and detailed mechanistic aspects of these catalytic

processes have been presented, the mechanisms of magnetic catalysis in aqueous medium have not been completely understood. A key point is that the determination of geometric and electronic structures of active species closely related to catalytic activities of magnetic catalysts is difficult. In addition, complicated interactions of reactive species with the magnetic materials often disturb the catalytic environment of the active center. As a result, it is difficult to obtain insights into the nature of the reaction and/or deactivation mechanisms. Thus, a future direction in this field is the use of advanced spectroscopic techniques such as synchrotron-based X-ray absorption, *in situ* synchrotron-based XPS, and IR microspectroscopy methods. Furthermore, computational studies may assist in providing valuable hints for understanding the interactions of the reactive species with the magnetic material. Detailed examinations and theoretical calculations, in turn, help in the design of highly efficient MRCs and in performing more challenging reactions. (2) In characterizations and evaluations, it should be noted that the types, sizes, and morphologies of prepared MRCs vary. In many cases, synthetic approaches involving multistep reactions are tedious and expensive. Thus, development of green prepared process with facile operation is more efficient and economical. Furthermore, characterization and evaluation of magnetic catalysts are often a challenging task because the magnetic nature of these catalysts poses difficulties in nuclear magnetic resonance technique, which often plays an important role in the determination of structures of active species. Therefore, the development of better characterization technique is another direction in this field. (3) Application of MRCs in industry is still at its infancy. The stability of MRCs is an important prerequisite for such application as it ensures feasibility and productivity of the application. Although inorganic shells have been shown to improve the stability and relatively easy and straightforward applications have been developed, exploration of the stability of MRCs is an unmet challenge. In addition, facile and scalable synthetic strategies are still in highly sought. Thus, future endeavors for more efficient protocols will still focus on the stability, sustainability, and environmental impact because of the growing needs of industry. These efforts enable a wide variety of industrial applications for magnetic catalysts in the future.

Acknowledgements

We are grateful to the Shanghai Sciences and Technologies Development Fund (13ZR1458700, 14jc1412300 and 12nm0500500), the Shanghai Municipal Education Commission (14YZ074, 12ZZ135, DXL122) and CSIRT (IRT1269) for financial support.

Notes and references

Key Laboratory of Resource Chemistry of Ministry of Education, Shanghai Key Laboratory of Rare Earth Functional Materials, Shanghai Normal University, Shanghai 200234, P. R. China. Tel: +86 21 64321819; E-mail: ghliu@shnu.edu.cn

1. R. A. Sheldon, *Chem. Commun.*, 2008, 3352-3365.
2. R. A. Sheldon and H. v. Bekkum, *Fine Chemicals through Heterogeneous Catalysis*, Wiley-VCH, Weinheim, 2001.
3. N. Lee and T. Hyeon, *Chem. Soc. Rev.*, 2012, **41**, 2575-2589.
4. D. Le Sage, K. Arai, D. R. Glenn, S. J. DeVience, L. M. Pham, L. Rahn-Lee, M. D. Lukin, A. Yacoby, A. Komeili and R. L. Walsworth, *Nature*, 2013, **496**, 486-489.
5. P. Moroz, S. K. Jones and B. N. Gray, *Int. J. Hyperther.*, 2002, **18**, 267-284.
6. A. Tomitaka, T. Yamada and Y. Takemura, *J. Nanomaterials*, 2012, **2012**, 1-5.
7. Q. Zhang, J. Tong, H. Chen, L. Jiang, H. Zhu, X. Zhu, H. Yu, J. Liu and B. Liu, *J. Nanosci. Nanotechnol.*, 2012, **12**, 127-131.
8. C. Binns, in *Nanostructured Materials for Magnetoelectronics*, eds. B. Aktaş and F. Mikailzade, Springer Berlin Heidelberg, 2013, vol. 175, ch. 8, pp. 197-215.
9. S. Shylesh, V. Schünemann and W. R. Thiel, *Angew. Chem. Int. Ed.*, 2010, **49**, 3428-3459.
10. M. B. Gawande, P. S. Branco and R. S. Varma, *Chem. Soc. Rev.*, 2013, **42**, 3371-3393.
11. A. Dhakshinamoorthy, S. Navalon, M. Alvaro and H. Garcia, *ChemSusChem*, 2012, **5**, 46-64.
12. C. W. Lim and I. S. Lee, *Nano Today*, 2010, **5**, 412-434.
13. D. Zhang, C. Zhou, Z. Sun, L.-Z. Wu, C.-H. Tung and T. Zhang, *Nanoscale*, 2012, **4**, 6244-6255.
14. V. Polshettiwar, R. Luque, A. Fihri, H. Zhu, M. Bouhrara and J.-M. Basset, *Chem. Rev.*, 2011, **111**, 3036-3075.
15. R. B. N. Baig and R. S. Varma, *Chem. Commun.*, 2013, **49**, 752-770.
16. H.-J. Xu, X. Wan, Y. Geng and X.-L. Xu, *Curr. Org. Chem.*, **17**, 1034-1050.
17. S. Byun, J. Chung, Y. Jang, J. Kwon, T. Hyeon and B. M. Kim, *RSC Adv.*, 2013, **3**, 16296-16299.
18. Y.-H. Liu, J. Deng, J.-W. Gao and Z.-H. Zhang, *Adv. Synth. Catal.*, 2012, **354**, 441-447.
19. V. Polshettiwar and R. S. Varma, *Org. Biomol. Chem.*, 2009, **7**, 37-40.
20. A.-H. Lu, W. Schmidt, N. Matoussevitch, H. Bönemann, B. Spliethoff, B. Tesche, E. Bill, W. Kiefer and F. Schüth, *Angew. Chem.*, 2004, **116**, 4403-4406.
21. B. Panella, A. Vargas and A. Baiker, *J. Catal.*, 2009, **261**, 88-93.
22. R. Arundhathi, D. Damodara, P. R. Likhar, M. L. Kantam, P. Saravanan, T. Magdaleno and S. H. Kwon, *Adv. Synth. Catal.*, 2011, **353**, 1591-1600.
23. J. Liu, X. Peng, W. Sun, Y. Zhao and C. Xia, *Org. Lett.*, 2008, **10**, 3933-3936.
24. R. Luque, B. Baruwati and R. S. Varma, *Green Chem.*, 2010, **12**, 1540-1543.
25. R. B. Nasir Baig and R. S. Varma, *Green Chem.*, 2012, **14**, 625-632.
26. D. Wang, L. Salmon, J. Ruiz and D. Astruc, *Chem. Commun.*, 2013, **49**, 6956-6958.
27. S. J. Hoseini, H. Nasrabadi, M. Azizi, A. S. Beni and R. Khalifeh, *Synthetic. Commun.*, 2012, **43**, 1683-1691.
28. R. Parella, Naveen, A. Kumar and S. A. Babu, *Tetrahedron Lett.*, 2013, **54**, 1738-1742.
29. J. S. Chen, C. Chen, J. Liu, R. Xu, S. Z. Qiao and X. W. Lou, *Chem. Commun.*, 2011, **47**, 2631-2633.
30. G. Li and L. Mao, *RSC Adv.*, 2012, **2**, 5108-5111.

31. S. Xuan, W. Jiang, X. Gong, Y. Hu and Z. Chen, *J. Phys. Chem. C*, 2008, **113**, 553-558.
32. A. Chanda and V. V. Fokin, *Chem. Rev.*, 2009, **109**, 725-748.
33. D. C. Rideout and R. Breslow, *J. Am. Chem. Soc.*, 1980, **102**, 7816-7817.
34. C. Loncaric, K. Manabe and S. Kobayashi, *Adv. Synth. Catal.*, 2003, **345**, 475-477.
35. D. Samanta, S. Mukherjee, Y. P. Patil and P. S. Mukherjee, *Chem. Eur. J.*, 2012, **18**, 12322-12329.
36. Z. Guan, J. Hu, Y. Gu, H. Zhang, G. Li and T. Li, *Green Chem.*, 2012, **14**, 1964-1970.
37. C. Liu, Y. Zhang, N. Liu and J. Qiu, *Green Chem.*, 2012, **14**, 2999-3003.
38. N. Liu, C. Liu and Z. Jin, *Green Chem.*, 2012, **14**, 592-597.
39. D. Gonzalez-Cruz, D. Tejedor, P. de Armas, E. Q. Morales and F. Garcia-Tellado, *Chem. Commun.*, 2006, 2798-2800.
40. F. Himo, T. Lovell, R. Hilgraf, V. V. Rostovtsev, L. Noodleman, K. B. Sharpless and V. V. Fokin, *J. Am. Chem. Soc.*, 2004, **127**, 210-216.
41. H. C. Kolb, M. G. Finn and K. B. Sharpless, *Angew. Chem. Int. Ed.*, 2001, **40**, 2004-2021.
42. G. de Almeida, E. M. Sletten, H. Nakamura, K. K. Palaniappan and C. R. Bertozzi, *Angew. Chem.*, 2012, **124**, 2493-2497.
43. N. P. Grimster, B. Stump, J. R. Fotsing, T. Weide, T. T. Talley, J. G. Yamauchi, Á. Nemezc, C. Kim, K.-Y. Ho, K. B. Sharpless, P. Taylor and V. V. Fokin, *J. Am. Chem. Soc.*, 2012, **134**, 6732-6740.
44. J. J. Gajewski, J. Jurajj, D. R. Kimbrough, M. E. Gande, B. Ganem and B. K. Carpenter, *J. Am. Chem. Soc.*, 1987, **109**, 1170-1186.
45. K. C. Nicolaou, H. Xu and M. Wartmann, *Angew. Chem. Int. Ed.*, 2005, **44**, 756-761.
46. Q. Lin, J. C. O'Neil and H. E. Blackwell, *Org. Lett.*, 2005, **7**, 4455-4458.
47. M. C. Pirrung and K. D. Sarma, *J. Am. Chem. Soc.*, 2003, **126**, 444-445.
48. N. Shapiro and A. Vigalok, *Angew. Chem. Int. Ed.*, 2008, **47**, 2849-2852.
49. C. de Graaff, E. Ruijter and R. V. A. Orru, *Chem. Soc. Rev.*, 2012, **41**, 3969-4009.
50. A. Dömling, W. Wang and K. Wang, *Chem. Rev.*, 2012, **112**, 3083-3135.
51. L. Kumar, T. Mahajan and D. D. Agarwal, *Green Chem.*, 2011, **13**, 2187-2196.
52. A. Podgoršek, S. Stavber, M. Zupan and J. Iskra, *Tetrahedron*, 2009, **65**, 4429-4439.
53. T. Matsuda, R. Yamanaka and K. Nakamura, *Tetrahedron: Asymmetry*, 2009, **20**, 513-557.
54. M. Mifsud, K. V. Parkhomenko, I. W. C. E. Arends and R. A. Sheldon, *Tetrahedron*, 2010, **66**, 1040-1044.
55. A. Ohtaka, Y. Kono, S. Inui, S. Yamamoto, T. Ushiyama, O. Shimomura and R. Nomura, *J. Mol. Catal. A Chem.*, 2012, **360**, 48-53.
56. M.-O. Simon and C.-J. Li, *Chem. Soc. Rev.*, 2012, **41**, 1415-1427.
57. R. N. Butler and A. G. Coyne, *Chem. Rev.*, 2010, **110**, 6302-6337.
58. S. Minakata and M. Komatsu, *Chem. Rev.*, 2008, **109**, 711-724.
59. C. I. Herreras, X. Yao, Z. Li and C.-J. Li, *Chem. Rev.*, 2007, **107**, 2546-2562.
60. D. Dallinger and C. O. Kappe, *Chem. Rev.*, 2007, **107**, 2563-2591.
61. C.-J. Li and L. Chen, *Chem. Soc. Rev.*, 2006, **35**, 68-82.
62. C.-J. Li, *Chem. Rev.*, 2005, **105**, 3095-3166.
63. R. Breslow, *Acc. Chem. Res.*, 2004, **37**, 471-478.
64. U. M. Lindström, *Chem. Rev.*, 2002, **102**, 2751-2772.
65. W. P. Jencks, *Chem. Rev.*, 1972, **72**, 705-718.
66. R. Breslow, *Acc. Chem. Res.*, 1991, **24**, 159-164.
67. J. Liu, S. Z. Qiao, Q. H. Hu and G. Q. Lu, *Small*, 2011, **7**, 425-443.
68. L. H. Reddy, J. L. Arias, J. Nicolas and P. Couvreur, *Chem. Rev.*, 2012, **112**, 5818-5878.
69. Q. Dai and A. Nelson, *Chem. Soc. Rev.*, 2010, **39**, 4057-4066.
70. A. H. Lu, E. L. Salabas and F. Schuth, *Angew. Chem. Int. Ed.*, 2007, **46**, 1222-1244.
71. S. Laurent, D. Forge, M. Port, A. Roch, C. Robic, L. V. Elst and R. N. Muller, *Chem. Rev.*, 2008, **108**, 2064-2110.
72. D. Ho, X. Sun and S. Sun, *Acc. Chem. Res.*, 2011, **44**, 875-882.
73. N. A. Frey, S. Peng, K. Cheng and S. Sun, *Chem. Soc. Rev.*, 2009, **38**, 2532-2542.
74. M. Colombo, S. Carregal-Romero, M. F. Casula, L. Gutierrez, M. P. Morales, I. B. Boehm, J. T. Heverhagen, D. Prospero and W. J. Parak, *Chem. Soc. Rev.*, 2012, **41**, 4306-4334.
75. S. Chen, Y. Hong, Y. Liu, J. Liu, C. W. T. Leung, M. Li, R. T. K. Kwok, E. Zhao, J. W. Y. Lam, Y. Yu and B. Z. Tang, *J. Am. Chem. Soc.*, 2013, **135**, 4926-4929.
76. Q. Chen, A. J. Rondinone, B. C. Chakoumakos and Z. John Zhang, *J. Magn. Magn. Mater.*, 1999, **194**, 1-7.
77. S.-J. Lee, J.-R. Jeong, S.-C. Shin, J.-C. Kim and J.-D. Kim, *J. Magn. Magn. Mater.*, 2004, **282**, 147-150.
78. A. B. Chin and I. I. Yaacob, *J. Mater. Process. Technol.*, 2007, **191**, 235-237.
79. L. Liz, M. A. López Quintela, J. Mira and J. Rivas, *J. Mater. Sci.*, 1994, **29**, 3797-3801.
80. J. A. López Pérez, M. A. López Quintela, J. Mira, J. Rivas and S. W. Charles, *J. Phys. Chem. B*, 1997, **101**, 8045-8047.
81. D. Chen and R. Xu, *Mater. Res. Bull.*, 1998, **33**, 1015-1021.
82. J. Wan, X. Chen, Z. Wang, X. Yang and Y. Qian, *J. Cryst. Growth*, 2005, **276**, 571-576.
83. L. M. Lacroix, N. F. Huls, D. Ho, X. L. Sun, K. Cheng and S. H. Sun, *Nano Lett.*, 2011, **11**, 1641-1645.
84. N. Miguel-Sancho, O. Bomati-Miguel, A. G. Roca, G. Martinez, M. Arruebo and J. Santamaria, *Ind. Eng. Chem. Res.*, 2012, **51**, 8348-8357.
85. M. Niederberger, *Acc. Chem. Res.*, 2007, **40**, 793-800.
86. L. Durães, B. F. O. Costa, J. Vasques, J. Campos and A. Portugal, *Mater. Lett.*, 2005, **59**, 859-863.
87. S. Ammar, A. Helfen, N. Jouini, F. Fievet, I. Rosenman, F. Villain, P. Molinie and M. Danot, *J. Mater. Chem.*, 2001, **11**, 186-192.
88. F. Fievet, J. P. Lagier, B. Blin, B. Beaudoin and M. Figlarz, *Solid State Ionics*, 1989, **32-33**, 198-205.
89. R. J. Joseyphus, D. Kodama, T. Matsumoto, Y. Sato, B. Jeyadevan and K. Tohji, *J. Magn. Magn. Mater.*, 2007, **310**, 2393-2395.
90. K. S. Suslick, M. Fang and T. Hyeon, *J. Am. Chem. Soc.*, 1996, **118**, 11960-11961.
91. R. Abu Mukh-Qasem and A. Gedanken, *J. Colloid Interface Sci.*, 2005, **284**, 489-494.

92. E. Hee Kim, H. Sook Lee, B. Kook Kwak and B.-K. Kim, *J. Magn. Magn. Mater.*, 2005, **289**, 328-330.
93. M. P. Morales, O. Bomati-Miguel, R. Pérez de Alejo, J. Ruiz-Cabello, S. Veintemillas-Verdaguer and K. O'Grady, *J. Magn. Magn. Mater.*, 2003, **266**, 102-109.
94. V.-V. Sabino, M. Maria del Puerto, B.-M. Oscar, B. Carmen, Z. Xinqing, B. Pierre, A. Rigoberto Pérez de, R.-C. Jesus, S. Martin, J. T.-C. Francisco and F. Joaquin, *J. Phys. D Appl. Phys.*, 2004, **37**, 2054-2059.
95. S. Veintemillas-Verdaguer, M. P. Morales and C. J. Serna, *Mater. Lett.*, 1998, **35**, 227-231.
96. S. Laurent, D. Forge, M. Port, A. Roch, C. Robic, L. Vander Elst and R. N. Muller, *Chem. Rev.*, 2008, **108**, 2064-2110.
97. C. Graf, D. L. J. Vossen, A. Imhof and A. van Blaaderen, *Langmuir*, 2003, **19**, 6693-6700.
98. W. Stöber, A. Fink and E. Bohn, *J. Colloid Interface Sci.*, 1968, **26**, 62-69.
99. M. Ohmori and E. Matijević, *J. Colloid Interface Sci.*, 1993, **160**, 288-292.
100. P. Tartaj and C. J. Serna, *J. Am. Chem. Soc.*, 2003, **125**, 15754-15755.
101. P. Tartaj, T. González-Carreño and C. J. Serna, *Adv. Mater.*, 2001, **13**, 1620-1624.
102. P. Tartaj, T. González-Carreño and C. J. Serna, *Langmuir*, 2002, **18**, 4556-4558.
103. C. T. Kresge, M. E. Leonowicz, W. J. Roth, J. C. Vartuli and J. S. Beck, *Nature*, 1992, **359**, 710-712.
104. Y. Deng, C. Deng, D. Qi, C. Liu, J. Liu, X. Zhang and D. Zhao, *Adv. Mater.*, 2009, **21**, 1377-1382.
105. Y. Deng, C. Wang, X. Shen, W. Yang, L. Jin, H. Gao and S. Fu, *Chem. Eur. J.*, 2005, **11**, 6006-6013.
106. F. Erogbogbo, K.-T. Yong, R. Hu, W.-C. Law, H. Ding, C.-W. Chang, P. N. Prasad and M. T. Swihart, *ACS Nano*, 2010, **4**, 5131-5138.
107. Y. Deng, Y. Cai, Z. Sun, J. Liu, C. Liu, J. Wei, W. Li, C. Liu, Y. Wang and D. Zhao, *J. Am. Chem. Soc.*, 2010, **132**, 8466-8473.
108. S. Giri, B. G. Trewyn, M. P. Stellmaker and V. S. Y. Lin, *Angew. Chem. Int. Ed.*, 2005, **44**, 5038-5044.
109. M. Ohmori and E. Matijević, *J. Colloid Interface Sci.*, 1992, **150**, 594-598.
110. W. Zhao, J. Gu, L. Zhang, H. Chen and J. Shi, *J. Am. Chem. Soc.*, 2005, **127**, 8916-8917.
111. Y. Deng, D. Qi, C. Deng, X. Zhang and D. Zhao, *J. Am. Chem. Soc.*, 2007, **130**, 28-29.
112. S. Inagaki, S. Guan, Y. Fukushima, T. Ohsuna and O. Terasaki, *J. Am. Chem. Soc.*, 1999, **121**, 9611-9614.
113. T. Asefa, M. J. MacLachlan, N. Coombs and G. A. Ozin, *Nature*, 1999, **402**, 867-871.
114. B. J. Melde, B. T. Holland, C. F. Blanford and A. Stein, *Chem. Mater.*, 1999, **11**, 3302-3308.
115. L. Zhang, S. Z. Qiao, Y. G. Jin, Z. G. Chen, H. C. Gu and G. Q. Lu, *Adv. Mater.*, 2008, **20**, 805-809.
116. C. X. Lin, Z. Li, S. Brumbley, L. Petrasovits, R. McQualter, C. Yu and G. Q. Lu, *J. Mater. Chem.*, 2011, **21**, 7565-7571.
117. J. Li, Y. Wei, W. Li, Y. Deng and D. Zhao, *Nanoscale*, 2012, **4**, 1647-1651.
118. Z. Zhang, H. Duan, S. Li and Y. Lin, *Langmuir*, 2010, **26**, 6676-6680.
119. Z. Wang, H. Guo, Y. Yu and N. He, *J. Magn. Magn. Mater.*, 2006, **302**, 397-404.
120. L. Kong, X. Lu, X. Bian, W. Zhang and C. Wang, *Acs Appl. Mater. Interfaces*, 2010, **3**, 35-42.
121. A.-H. Lu, W.-C. Li, N. Matoussevitch, B. Spliethoff, H. Bonnemann and F. Schuth, *Chem. Commun.*, 2005, 98-100.
122. M. Zhu and G. Diao, *J. Phys. Chem. C*, 2011, **115**, 24743-24749.
123. S. C. Tsang, V. Caps, I. Paraskevas, D. Chadwick and D. Thompsett, *Angew. Chem. Int. Ed.*, 2004, **43**, 5645-5649.
124. K. H. Ang, I. Alexandrou, N. D. Mathur, G. A. J. Amaratunga and S. Haq, *Nanotechnology*, 2004, **15**, 520-524.
125. J. Lin, W. Zhou, A. Kumbhar, J. Wiemann, J. Fang, E. E. Carpenter and C. J. O'Connor, *J. Solid State Chem.*, 2001, **159**, 26-31.
126. T. Teranishi and M. Miyake, *Chem. Mater.*, 1999, **11**, 3414-3416.
127. C.-H. Jun, Y. J. Park, Y.-R. Yeon, J.-r. Choi, W.-r. Lee, S.-j. Ko and J. Cheon, *Chem. Commun.*, 2006, 1619-1621.
128. L. Wang, J. Luo, M. M. Maye, Q. Fan, Q. Rendeng, M. H. Engelhard, C. Wang, Y. Lin and C.-J. Zhong, *J. Mater. Chem.*, 2005, **15**, 1821-1832.
129. C. Xu, J. Xie, D. Ho, C. Wang, N. Kohler, E. G. Walsh, J. R. Morgan, Y. E. Chin and S. Sun, *Angew. Chem. Int. Ed.*, 2008, **47**, 173-176.
130. M.-C. Daniel and D. Astruc, *Chem. Rev.*, 2003, **104**, 293-346.
131. Y. Lee, M. A. Garcia, N. A. Frey Huls and S. Sun, *Angew. Chem. Int. Ed.*, 2010, **49**, 1271-1274.
132. S.-J. Cho, J.-C. Idrobo, J. Olamit, K. Liu, N. D. Browning and S. M. Kauzlarich, *Chem. Mater.*, 2005, **17**, 3181-3186.
133. R. D. Rieke, *Acc. Chem. Res.*, 1977, **10**, 301-306.
134. Z. Ban, Y. A. Barnakov, F. Li, V. O. Golub and C. J. O'Connor, *J. Mater. Chem.*, 2005, **15**, 4660-4662.
135. C. R. Vestal and Z. J. Zhang, *J. Am. Chem. Soc.*, 2002, **124**, 14312-14313.
136. G. Li, J. Fan, R. Jiang and Y. Gao, *Chem. Mater.*, 2004, **16**, 1835-1837.
137. N. Pothayee, S. Balasubramaniam, R. M. Davis, J. S. Riffle, M. R. J. Carroll, R. C. Woodward and T. G. St. Pierre, *Polymer*, 2011, **52**, 1356-1366.
138. L. Lei, X. Liu, Y. Li, Y. Cui, Y. Yang and G. Qin, *Mater. Chem. Phys.*, 2011, **125**, 866-871.
139. Hu, K. G. Neoh, L. Cen and E.-T. Kang, *Biomacromolecules*, 2006, **7**, 809-816.
140. A. R. Herdt, B.-S. Kim and T. A. Taton, *Bioconjugate Chem.*, 2006, **18**, 183-189.
141. M. A. Kadir, S. J. Kim, E.-J. Ha, H. Y. Cho, B.-S. Kim, D. Choi, S.-G. Lee, B. G. Kim, S.-W. Kim and H.-j. Paik, *Adv. Funct. Mater.*, 2012, **22**, 4032-4037.
142. S. A. Corr, Y. K. Gun'ko, A. P. Douvalis, M. Venkatesan, R. D. Gunning and P. D. Nellist, *J. Phys. Chem. C*, 2008, **112**, 1008-1018.
143. S. Narayan, J. Muldoon, M. G. Finn, V. V. Fokin, H. C. Kolb and K. B. Sharpless, *Angew. Chem. Int. Ed.*, 2005, **44**, 3275-3279.
144. B. Karami, S. J. Hoseini, K. Eskandari, A. Ghasemi and H. Nasrabadi, *Catal. Sci. Technol.*, 2012, **2**, 331-338.
145. S. Pagoti, S. Surana, A. Chauhan, B. Parasar and J. Dash, *Catal. Sci. Technol.*, 2013, **3**, 584-588.
146. J. Safari, Z. Zarnegar and M. Heydarian, *B. Chem. Soc. Jpn.*, 2012, **85**, 1332-1338.

- 147.S. Rostamnia, A. Nuri, H. Xin, A. Pourjavadi and S. H. Hosseini, *Tetrahedron Lett.*, 2013, **54**, 3344-3347.
- 148.S. R. Kale, S. S. Kahandal, M. B. Gawande and R. V. Jayaram, *RSC Adv.*, 2013, **3**, 8184-8192.
- 149.F. Rajabi, N. Karimi, M. R. Saidi, A. Primo, R. S. Varma and R. Luque, *Adv. Synth. Catal.*, 2012, **354**, 1707-1711.
- 150.K. Shin, J.-Y. Choi, C. Park, H. Jang and K. Kim, *Catal. Lett.*, 2009, **133**, 1-7.
- 151.X. Zhang, W. Jiang, X. Gong and Z. Zhang, *J. Alloy. Compd.*, 2010, **508**, 400-405.
- 152.Y. Chi, Q. Yuan, Y. Li, J. Tu, L. Zhao, N. Li and X. Li, *J. Colloid Interface Sci.*, 2012, **383**, 96-102.
- 153.G. Dang, Y. Shi, Z. Fu and W. Yang, *Chinese J. Catal.*, 2012, **33**, 651-658.
- 154.M. Zhu, C. Wang, D. Meng and G. Diao, *J. Mater. Chem. A*, 2013, **1**, 2118-2125.
- 155.Y. Wu, T. Zhang, Z. Zheng, X. Ding and Y. Peng, *Mater. Res. Bull.*, 2010, **45**, 513-517.
- 156.J. Zheng, Y. Dong, W. Wang, Y. Ma, J. Hu, X. Chen and X. Chen, *Nanoscale*, 2013, **5**, 4894-4901.
- 157.H. Zhang and X.-l. Yang, *Chin. J. Polym. Sci.*, 2011, **29**, 342-351.
- 158.Y. Zhu, J. Shen, K. Zhou, C. Chen, X. Yang and C. Li, *J. Phys. Chem. C*, 2010, **115**, 1614-1619.
- 159.T. Zeng, X. Zhang, S. Wang, Y. Ma, H. Niu and Y. Cai, *J. Mater. Chem. A*, 2013, **1**, 11641-11647.
- 160.J. Hu, Y.-l. Dong, X.-j. Chen, H.-j. Zhang, J.-m. Zheng, Q. Wang and X.-g. Chen, *Chem. Eng. J.*, 2014, **236**, 1-8.
- 161.V. K. Gupta, N. Atar, M. L. Yola, Z. Üstündağ and L. Uzun, *Water Res.*, 2014, **48**, 210-217.
- 162.J. Ge, T. Huynh, Y. Hu and Y. Yin, *Nano Lett.*, 2008, **8**, 931-934.
- 163.X. Miao, T. Wang, F. Chai, X. Zhang, C. Wang and W. Sun, *Nanoscale*, 2011, **3**, 1189-1194.
- 164.F. Zhang, N. Liu, P. Zhao, J. Sun, P. Wang, W. Ding, J. Liu, J. Jin and J. Ma, *Appl. Surf. Sci.*, 2012, **263**, 471-475.
- 165.A. Rezaeifard, M. Jafarpour, A. Naeimi and R. Haddad, *Green Chem.*, 2012, **14**, 3386-3394.
- 166.R. Hudson, C.-J. Li and A. Moores, *Green Chem.*, 2012, **14**, 622-624.
- 167.R. B. Nasir Baig and R. S. Varma, *Green Chem.*, 2013, **15**, 398-417.
- 168.X. Xiong and L. Cai, *Catal. Sci. Technol.*, 2013, **3**, 1301-1307.
- 169.H. Wang, W. Zhang, B. Shentu, C. Gu and Z. Weng, *J. Appl. Polym. Sci.*, 2012, **125**, 3730-3736.
- 170.B. S. P. Anil Kumar, K. Harsha Vardhan Reddy, B. Madhav, K. Ramesh and Y. V. D. Nageswar, *Tetrahedron Lett.*, 2012, **53**, 4595-4599.
- 171.A. S. Kumar, M. A. Reddy, M. Knorn, O. Reiser and B. Sreedhar, *Eur. J. Org. Chem.*, 2013, **2013**, 4674-4680.
- 172.M. Kaya, M. Zahmakiran, S. Özkaz and M. Volkan, *Acs Appl. Mater. Interfaces*, 2012, **4**, 3866-3873.
- 173.A. Rezaeifard, M. Jafarpour, P. Farshid and A. Naeimi, *Eur. J. Inorg. Chem.*, 2012, **2012**, 5515-5524.
- 174.H. Naeimi, Z. Rashid, A. H. Zarnani and R. Ghahremanzadeh, *New J. Chem.*, 2014, **38**, 348-357.
- 175.R. Ghahremanzadeh, Z. Rashid, A. H. Zarnani and H. Naeimi, *Appl. Catal. A: Gen.*, 2013, **467**, 270-278.
- 176.Z. Ji, X. Shen, G. Zhu, H. Zhou and A. Yuan, *J. Mater. Chem.*, 2012, **22**, 3471-3477.
- 177.M. H. Rashid, M. Raula and T. K. Mandal, *J. Mater. Chem.*, 2011, **21**, 4904-4917.
- 178.E. Weiss, B. Dutta, Y. Schnell and R. Abu-Reziq, *J. Mater. Chem. A*, 2014, **2**, 3971-3977.
- 179.S. Fujii, H. Hamasaki, H. Abe, S. Yamanaka, A. Ohtaka, E. Nakamura and Y. Nakamura, *J. Mater. Chem. A*, 2013, **1**, 4427-4430.
- 180.M. A. Zolfigol, V. Khakyzadeh, A. R. Moosavi-Zare, A. Rostami, A. Zare, N. Iranpoor, M. H. Beyzavi and R. Luque, *Green Chem.*, 2013, **15**, 2132-2140.
- 181.A. Saha, J. Leazer and R. S. Varma, *Green Chem.*, 2012, **14**, 67-71.
- 182.K. Mori, N. Yoshioka, Y. Kondo, T. Takeuchi and H. Yamashita, *Green Chem.*, 2009, **11**, 1337-1342.
- 183.S. Wu, J. Kaiser, X. Guo, L. Li, Y. Lu and M. Ballauff, *Ind. Eng. Chem. Res.*, 2012, **51**, 5608-5614.
- 184.B. Dong, D. L. Miller and C. Y. Li, *J. Phys. Chem. Lett.*, 2012, **3**, 1346-1350.
- 185.V. Polshettiwar and R. S. Varma, *Chem. Eur. J.*, 2009, **15**, 1582-1586.
- 186.R. B. N. Baig and R. S. Varma, *Chem. Commun.*, 2012, **48**, 6220-6222.
- 187.S. E. Garcia-Garrido, J. Francos, V. Cadierno, J.-M. Basset and V. Polshettiwar, *ChemSusChem*, 2011, **4**, 104-111.
- 188.U. Laska, C. Frost, P. Plucinski and G. Price, *Catal. Lett.*, 2008, **122**, 68-75.
- 189.G. Liu, H. Gu, Y. Sun, J. Long, Y. Xu and H. Li, *Adv. Synth. Catal.*, 2011, **353**, 1317-1324.
- 190.Y. Sun, G. Liu, H. Gu, T. Huang, Y. Zhang and H. Li, *Chem. Commun.*, 2011, **47**, 2583-2585.
- 191.X. Gao, R. Liu, D. Zhang, M. Wu, T. Cheng and G. Liu, *Chem. Eur. J.*, 2014, **20**, 1515-1519.
- 192.J. Li, Y. Zhang, D. Han, Q. Gao and C. Li, *J. Mol. Catal. A Chem.*, 2009, **298**, 31-35.
- 193.F.-P. Ma, P.-H. Li, B.-L. Li, L.-P. Mo, N. Liu, H.-J. Kang, Y.-N. Liu and Z.-H. Zhang, *Appl. Catal. A: Gen.*, 2013, **457**, 34-41.
- 194.E. Rafiee and S. Eavani, *Green Chem.*, 2011, **13**, 2116-2122.
- 195.E. Rafiee, S. Eavani and M. Khodayari, *Chinese J. Catal.*, 2013, **34**, 1513-1518.
- 196.Y. Zheng, C. Duanmu and Y. Gao, *Org. Lett.*, 2006, **8**, 3215-3217.
- 197.V. Polshettiwar, B. Baruwati and R. S. Varma, *Chem. Commun.*, 2009, 1837-1839.
- 198.V. Polshettiwar and R. S. Varma, *Tetrahedron*, 2010, **66**, 1091-1097.
- 199.F. Nemati, M. M. Heravi and R. Saeedi Rad, *Chinese J. Catal.*, 2012, **33**, 1825-1831.
- 200.F. Nemati and R. Saedirad, *Chin. Chem. Lett.*, 2013, **24**, 370-372.
- 201.J. Deng, L.-P. Mo, F.-Y. Zhao, Z.-H. Zhang and S.-X. Liu, *ACS Comb. Sci.*, 2012, **14**, 335-341.
- 202.H. Guo, Y. Lian, L. Yan, X. Qi and R. L. Smith, *Green Chem.*, 2013, **15**, 2167-2174.
- 203.C. Zhang, H. Wang, F. Liu, L. Wang and H. He, *Cellulose*, 2013, **20**, 127-134.
- 204.A. Rostami, B. Tahmasbi, H. Gholami and H. Taymorian, *Chin. Chem. Lett.*, 2013, **24**, 211-214.
- 205.M. Khoobi, L. Ma'mani, F. Rezazadeh, Z. Zareie, A. Foroumadi, A. Ramazani and A. Shafiee, *J. Mol. Catal. A Chem.*, 2012, **359**, 74-80.
- 206.Y. Kong, R. Tan, L. Zhao and D. Yin, *Green Chem.*, 2013, **15**, 2422-2433.

ARTICLE

- 207.J. Davarpanah, A. R. Kiasat, S. Noorzadeh and M. Ghahremani, *J. Mol. Catal. A Chem.*, 2013, **376**, 78-89.
- 208.B. Karimi and E. Farhangi, *Chem. Eur. J.*, 2011, **17**, 6056-6060.
- 209.A. R. Kiasat and S. Nazari, *J. Mol. Catal. A Chem.*, 2012, **365**, 80-86.
- 210.A. Kiasat and S. Nazari, *J. Incl. Phenom. Macrocycl. Chem.*, 2013, **76**, 363-368.
- 211.J. Zhu, P. Wang; and M. Lu, *J. Braz. Chem. Soc.*, 2013, **24**, 171-176.
- 212.D. Damodara, R. Arundhathi and P. R. Likhar, *Catal. Sci. Technol.*, 2013, **3**, 797-802.
- 213.M. S. Saeedi, S. Tangestaninejad, M. Moghadam, V. Mirkhani, I. Mohammadpoor-Baltork and A. R. Khosropour, *Polyhedron*, 2013, **49**, 158-166.
- 214.Y. Wang, P. Jiang, W. Zhang and J. Zheng, *Appl. Surf. Sci.*, 2013, **270**, 531-538.
- 215.Z. Wang, P. Xiao, B. Shen and N. He, *Colloids Surf. A: Physicochem. Eng. Asp.*, 2006, **276**, 116-121.
- 216.J. Wang, B. Xu, H. Sun and G. Song, *Tetrahedron Lett.*, 2013, **54**, 238-241.
- 217.Q. Du, W. Zhang, H. Ma, J. Zheng, B. Zhou and Y. Li, *Tetrahedron*, 2012, **68**, 3577-3584.
- 218.Y. Jiang, Q. Gao, M. Ruan, H. Yu and L. Qi, *Nanotechnology*, 2008, **19**, 075714.
- 219.Q. Zhang, H. Su, J. Luo and Y. Wei, *Catal. Sci. Technol.*, 2013, **3**, 235-243.
- 220.M. Ghotbinejad, A. R. Khosropour, I. Mohammadpoor-Baltork, M. Moghadam, S. Tangestaninejad and V. Mirkhani, *J. Mol. Catal. A Chem.*, 2014, **385**, 78-84.
- 221.S. Xuan, W. Jiang and X. Gong, *Dalton. Trans.*, 2011, **40**, 7827-7830.
- 222.B. R. Vaddula, A. Saha, J. Leazer and R. S. Varma, *Green Chem.*, 2012, **14**, 2133-2136.
- 223.M. Shokouhimehr, J. E. Lee, S. I. Han and T. Hyeon, *Chem. Commun.*, 2013, **49**, 4779-4781.
- 224.M. Keller, V. Collière, O. Reiser, A.-M. Caminade, J.-P. Majoral and A. Ouali, *Angew. Chem. Int. Ed.*, 2013, **52**, 3626-3629.
- 225.D. Lee, J. Lee, H. Lee, S. Jin, T. Hyeon and B. M. Kim, *Adv. Synth. Catal.*, 2006, **348**, 41-46.
- 226.M. Kawamura and K. Sato, *Chem. Commun.*, 2006, 4718-4719.
- 227.A. Alizadeh, M. M. Khodaei, M. Beygzadeh, D. Kordestani and M. Feyzi, *B. Kor. Chem. Soc.*, 2012, **33**, 2546-2552.
- 228.H.-J. Xu, X. Wan, Y.-Y. Shen, S. Xu and Y.-S. Feng, *Org. Lett.*, 2012, **14**, 1210-1213.